

國立台灣大學醫學院分子醫學研究所



博士論文

Institute of Molecular Medicine
College of Medicine
National Taiwan University
Doctoral Dissertation

RBM4 藉由調控丙酮酸激酶之選擇性剪接

促進間質性幹細胞之神經分化

RBM4 regulates neuronal differentiation of mesenchymal
stem cells by modulating alternative splicing of
Pyruvate kinase M

蘇俊豪

Chun-Hao Su

指導教授：譚婉玉 教授

Advisor: Woan-Yuh Tarn, PhD

中華民國 106 年 6 月

June 2017

目錄

口試委員會審定書.....	i
誌謝.....	ii
中文摘要.....	iii
Abstract.....	iv
1. Introduction.....	1
1.1. Role of alternative splicing in self-renewal and differentiation of stem cells.....	1
1.2. Alternative splicing regulates neuronal differentiation and neurologic functions.....	2
1.3. RNA-binding protein 4 (RBM4) and its role in cell differentiation.....	4
1.4. Pyruvate kinase M (PKM) and its role in metabolic regulation and cell differentiation.....	5
1.5. Regulation of energy metabolism in self-renewal and differentiation of stem cells.....	8
1.6. Mesenchymal stem cells (MSCs) and its metabolic properties.....	10
2. Results.....	13
2.1 Pkm isoform switched during mouse embryo development in brain, heart and muscle.....	13
2.2 RBM4 significantly affects Pkm isoform switch in highly energy-consuming tissues.....	14
2.3 Mechanism of RBM4-regulated PKM isoform expression.....	14
2.3.1 RBM4 regulates alternative splicing of PKM not by suppressing PTB protein expression.....	14
2.3.2 RBM4 regulates alternative splicing of PKM pre-mRNA via an intronic CU-rich sequence.....	15
2.4. RBM4 is involved in the PKM isoform switch during neuronal differentiation of human MSCs.....	16
2.5. RBM4 promotes neuronal differentiation and neurite outgrowth of MSCs.....	18
2.6. RBM4-regulated PKM1 isoform expression enhances mitochondrial OXPHOS and promotes neuronal differentiation of MSCs.....	19
2.7. RBM4 promotes neuronal differentiation via suppressing a negative regulating pathway.....	21
2.8. Hypoxia environment induces RBM4 expression and neuronal differentiation of MSCs.....	22





2.9. RBM4 is involved in the hypoxia-induced switch of PKM splicing isoforms and neuronal differentiation.....	23
2.10. RBM4 induces the expression of a PTB isoform with attenuated activity in human MSCs.....	24
3. Discussion.....	27
3.1. RBM4 directly modulates PKM isoform switch in the developing brain.....	27
3.2. The RBM4-mediated PKM isoform shift contributes to neuronal differentiation.....	28
3.3. RBM4 regulates neuronal differentiation and neuronal function via various pathways.....	31
3.4. Hypoxia induces neuronal differentiation via the RBM4-mediated PKM isoform shift.....	32
3.5. RBM4 regulates PTB isoform expression and suppresses PTB activity in MSCs.....	33
4. Materials and Methods.....	37
Reference.....	44
Figures.....	58
Table.....	76



國立臺灣大學博士學位論文
口試委員會審定書

RBM4 藉由調控丙酮酸激酶 M 型之選擇性剪接
促進間質性幹細胞之神經分化
RBM4 regulates neuronal differentiation of
mesenchymal stem cells by modulating alternative
splicing of pyruvate kinase M

本論文係 蘇俊豪 君 (D00448006) 在國立臺灣大學醫學院分子醫學研究所完成之博士學位論文，於民國 106 年 1 月 12 日承下列考試委員審查通過及口試及格，特此證明

口試委員：

蘇俊豪

(簽名)

(指導教授)

黃兆瑩

李思仁

王松馨

洪士杰

系主任、所長

李思仁

(簽名)

(是否須簽章依各院系所規定)



誌謝

漫長的博士班時光，終於在這篇小小的博士論文完稿後，完成了一個階段。雖然這僅是未來漫長研究生涯中的一小段路，然而，卻也是付出了相當多心血的結晶。同時，在這段期間也受到相當多的鼓勵與支持。因此在這以一段致謝表達感謝之意。

首先，需要感謝的是我的博士班論文指導教授，譚婉玉老師。老師對於研究上的投入與專注，令人尊敬不已。對於立志從事研究工作的我們無異是個學習的榜樣。而老師鼓勵我們積極的參與學術活動、隨時的接受新知，都是促進我們培育專業研究能力的好方法。在博士研究期間，也感謝老師對於研究方向的指導與協助。在不斷的討論中逐漸培養獨立思考與研究的能力。

同時，也需要感謝我的論文指導委員：李芳仁老師、黃怡萱老師、王桂馨老師以及洪士杰老師。感謝老師們在我的研究過程中提出的疑問以及可行的研究方向，使這篇論文能夠更臻完整。老師們對於研究中，盲點的發掘與對於疑問謹慎的態度亦是我未來研究時的楷模。

另外，感謝實驗室的夥伴們。感謝學長姊細心以及非常有耐心的教導我許多實驗上的知識，不論是技術的分享、觀念的傳授、問題的發現與解決。也感謝同學以及學弟妹們的支援與忍耐，包容任性的我，並且為漫長的研究生活中增添極多的樂趣。

最後也是最需要感謝的莫過總是支持我的家人。在研究生活中，經常會有只能專注在實驗上的時刻，感謝你們對我的諒解，提供我一個無後顧之憂的環境。也感謝父母總是尊重我的每一個決定：做我想做的事，追求我想達成的目標。感謝你們。

中文摘要



mRNA 的選擇性剪接對大腦的發育以及神經功能有重要的影響。RBM4 可透過調控選擇性剪接促進神經前驅細胞的分化及培養中神經細胞突觸的生長。本論文中，我進一步的探討 RBM4 在神經分化過程中扮演的角色。在神經分化過程中，能量產生路徑由醣解作用改變為氧化磷酸化作用。我發現在腦部發育過程中，醣解代謝酵素丙酮酸激酶(PKM)的選擇性剪接會使酵素由 M2 型變為 M1 型。同時，我觀察到在小鼠胚胎腦中，單一 Rbm4 基因的剔除會影響此酵素異構物的轉變。在間質性幹細胞(Mesenchymal stem cells; MSCs)的神經分化過程中，亦會發生此一選擇性剪接作用。利用 PKM minigene，我證實 RBM4 能直接調控此一選擇性剪接作用。在 MSC 中過量表達 RBM4 或是 PKM1 可以誘導神經相關基因的表現，同時亦能增加細胞的粒線體呼吸作用並促進神經性分化。因此，在神經分化過程中，RBM4 對於 PKM 異構型的轉變以及其導致的能量代謝作用之改變扮演著重要的角色。此外，RBM4 所調控之 PKM 異構物轉變，也可能進一步影響細胞增生以及細胞內醣解作用相關酵素的表現。另外，此研究中我們亦發現在低氧促進 MSC 神經性分化過程中，RBM4 被誘導而增加其表現，並且進一步調控 PKM 異構物的轉變以及神經相關基因的表達。此結果顯示 RBM4 具有應用於神經性退化疾病治療的潛力。最後，我發現了在不同型態的細胞中，RBM4 藉由不同的機制影響另一個選擇性剪接調控分子 PTB 的表現。我證實了在 MSC 中，RBM4 可以拮抗 PTB 的作用並且影響其表現而產生一個具較弱抑制性的 PTB 異構物。因此，RBM4 透過改變不同選擇性剪接作用而在神經分化過程中扮演著重要的角色。本論文再證明了選擇性剪接在神經性分化或者是大腦發育過程中之重要性。

關鍵字：選擇性剪接、低氧、間質性幹細胞、神經性分化、丙酮酸激酶

Abstract



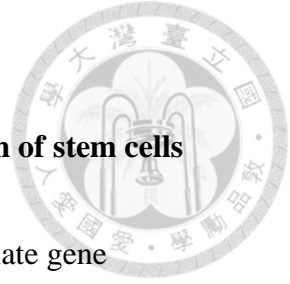
Brain development and neurologic functions involve numerous alternative splicing (AS) events. RBM4 promotes differentiation of neuronal progenitor cells and neurite outgrowth of cultured neurons via its role in splicing regulation. In this study, we further explored the role of RBM4 in neuronal differentiation. During neuronal differentiation, energy production shifts from glycolysis to oxidative phosphorylation. We found that the splice isoform change of the metabolic enzyme pyruvate kinase M (PKM) from PKM2 to PKM1 occurs during brain development and is impaired in RBM4-deficient brains. The PKM isoform change could be recapitulated in human mesenchymal stem cells (MSCs) during neuronal induction. Using a PKM minigene, we demonstrated that RBM4 plays a direct role in regulating alternative splicing of PKM. Overexpression of RBM4 or PKM1 induced the expression of neuronal genes, increased mitochondrial respiration capacity in MSCs, and, accordingly, promoted neuronal differentiation. Hence, RBM4 plays an important role in the PKM isoform switch and change in mitochondrial energy production during neuronal differentiation. In addition, RBM4-mediated isoform switch of PKM may affect cell proliferation and the expression of glycolytic enzymes. Moreover, we demonstrated that RBM4 is induced and is involved in the PKM splicing switch and

neuronal gene expression during hypoxia-induced neuronal differentiation. These results reveal the potential of RBM4 in therapeutic application of neurodegenerative diseases.



Finally, RBM4 regulates the expression of another critical splicing regulator PTB, which involves distinct mechanism among different cell types. We demonstrated that RBM4 antagonized the function of PTB and induced the expression of a PTB isoform with attenuated splicing activity in MSCs. Thus, RBM4 modulates neuronal differentiation essentially via its role in alternative splicing.

Key words: Alternative splicing, hypoxia, mesenchymal stem cells, neuronal differentiation, pyruvate kinase M

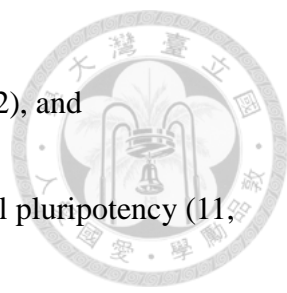


1. Introduction

1.1. Role of alternative splicing in self-renewal and differentiation of stem cells

Alternative splicing (AS) is one of the many processes that regulate gene expression in eukaryotic cells. AS selects different exons of precursor-mRNA (pre-mRNA) and increases cell complexity by generating proteins with different functions, or by changing the localization, translation or stability of mRNA in the cell (1, 2). Basically, the conserved *cis*-acting splicing signals include 5' and 3' splicing sites, and the branch site on the pre-mRNA guide the spliceosome assembling and further generate the intron removal (1). However, only using *cis*-acting elements may not be sufficient in the precise splicing site selection or proper AS regulation (3, 4). Indeed, the *trans*-acting splicing factors are critical in modulating the selection of exons via the recognition of specific RNA motifs. Moreover, the arrangement of RNA motifs, the modification of splicing factors, or the interactions between different cofactors also considerably affect AS (5, 6).

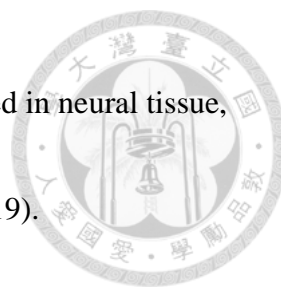
AS events involved in many cellular function regulation including modulation of signaling pathways or cell cycle (7). Moreover, many studies had identified the differential expression profiles between stem cells and differentiated cells (7-10). Fine turn of key transcription factors such as octamer-binding transcription factor 4 (OCT4),



Nanog homeobox (NANOG), sex determining region Y-box 2 (SOX2), and transcription factor 3 (TCF3) is important for stabilizing the stem cell pluripotency (11, 12). Interestingly, the isoform switch of TCF3 or OCT4 affects the self-renewal of stem cells (7, 9). Furthermore, a forkhead box (FOX) transcription factor, FOXP1, is critical for regulating the expression of several transcription factors, which control the pluripotency of stem cells (13). Recently, a study shows that expression of the ESC-specific FOXP1 isoform is regulated by AS. The switch of FOXP1 isoforms control the pluripotency and reprogramming of ESCs (14). Moreover, many splicing factors also shown the differentially expression pattern at different embryonic development stages, suggesting that the balance between self-renewal and differentiation of stem cells is highly regulated by AS events (15).

1.2. Alternative splicing regulates neuronal differentiation and neurologic functions

Studies using genome-wide analysis suggested that the widest AS events enriched in the neural and muscle tissues in vertebrates. Also, these studies indicated that the high AS frequencies contribute to the various functions of the nervous system (16, 17).



Moreover, several splicing regulators are specific- or highly expressed in neural tissue, and have huge effects on the neuronal development or disorder (18, 19).

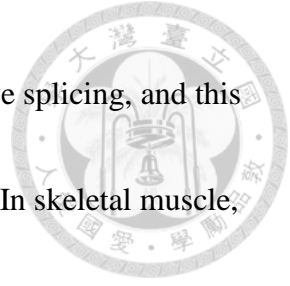
Splicing factors highly regulate most aspects of the neuronal development including neurogenesis and mature synaptic functions (19). During neurogenesis, the expression of a splicing factor, polypyrimidine tract binding protein 1 (PTBP1), gradually reduces. This reduction accompanied by the increment of another splicing factor, PTBP2 (nPTB) (20). PTBP1 and PTBP2 regulate different repertoires of AS events. PTBP1 suppresses the splicing of subset neural targets to inhibit neuronal differentiation, whereas PTBP2 activates the splicing of the neural targets to enhance neuronal differentiation (20). In addition, splicing factor serine/arginine repetitive matrix protein 4 (SRRM4/nSR100) is also important during neurogenesis by antagonizing the PTBP1 activity (19, 21). Indeed, throughout the development of nervous system, there are some other splicing factors regulate the AS events. For example, both RNA-binding protein fox-1 homolog (RBFOX) proteins and neuro-oncological ventral antigen (NOVA) proteins modulate the AS targets, which involves in the migration of neurons (22-25). Thus, proper expression of splicing factors is critical for brain development and neurological functions.

1.3. RNA-binding protein 4 (RBM4) and its role in cell differentiation



RBM4 is an RNA-binding protein with two RNA recognition motif (RRM) domains (26). The homolog of mammalian RBM4 was first identified as Lark in *Drosophila*. Lark is essential for embryonic development and the circadian regulation of adult eclosion (27). The human RBM4 is widely expressed in many tissues such as skeletal muscle, heart, frontal cortex and hippocampus of the brain (28, 29). Moreover, the mammalian RBM4 is involved in many mRNA regulatory processes including splicing, localization, and stability (28, 30).


RBM4 modulates the AS of pre-mRNAs, which participates in cell differentiation and tumorigenesis had been reported (31-35). Several studies revealed the role of RBM4 in the differentiation processes of muscle, pancreas and adipocytes (31-33). Actually, we recently reported that RBM4 is also involved in neuronal differentiation of mouse embryonal carcinoma P19 cells and neural progenitor-derived cells (34). RBM4 promotes the expression of Numb splice isoforms that function during neuronal differentiation and neurite outgrowth. However, the question of whether RBM4 regulates neuronal differentiation via modulating other AS events remains unclear.



The expression of splicing factors usually archived via alternative splicing, and this can be regulated by splicing factor itself or by other splicing factors. In skeletal muscle, RBM4 represses PTB protein expression via alternative splicing coupled non-sense mediated decay (AS-NMD) (31). Besides, RBM4 also antagonizes the splicing activity of PTB during myoblast differentiation (31). However, whether RBM4 also regulates neuronal differentiation via suppressing PTB is unclear. Intriguingly, RBM4 affects the alternative splicing of pyruvate kinase M (PKM) during neuronal differentiation of P19 cells (34). The PKM is one of the splicing targets of PTB in cancer cells. Thus, RBM4 may also regulate the PKM AS events during neuronal differentiation via modulating the expression or the splicing activity of PTB. In this study, I assessed whether or not RBM4 could modulate neuronal differentiation via suppressing PTB and further explored its underlying mechanism.

1.4. Pyruvate kinase M (PKM) and its role in metabolic regulation and cell differentiation

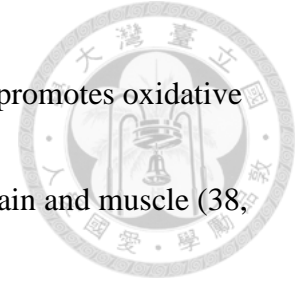
Pyruvate kinase (PK) regulates the final step of glycolysis, which converts phosphoenolpyruvate (PEP) to pyruvate, a critical leading step before either oxidative



phosphorylation of pyruvate or fermentation (36). In mammals, there are four isoforms (L, R, M1 and M2 type) exist in different tissues. The L gene encodes both PKL and PKR in the liver or red blood cells respectively and translates into protein by using different promoters (37). PKM1 and PKM2 are mutually exclusive spliced of exon 9 (PKM1) or exon 10 (PKM2) on M gene (38).

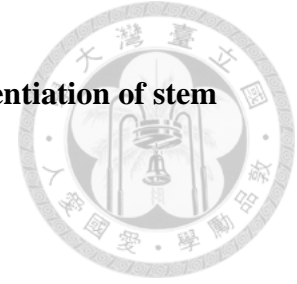
Unlike M1 isoform, the kinetic activity of L, R, and M2 isoforms allosterically regulated by binding with PEP, fructose-1,6-bisphosphate (FBP), metal, or ATP (36, 39). PKM2 contributes to intricate metabolic reprogramming through monomer-tetramer interconversion (40). However, all three forms of PKM2 are less efficient than PKM1 in PEP-pyruvate conversion. The tetramer form of PKM2 has a higher kinetic activity than the monomer. The monomer structure has nearly no enzymatic activity in converting PET into pyruvate. Instead, the low enzymatic activity allows cells using a fermentation pathway to generate lactate even in the presence of oxygen, which is called the Warburg effect (also defined as anabolic glycolysis) (40). The PKM2 also triggers other metabolic pathways and generates intermediate molecular such as nucleotides and amino acids (41). Thus, the dynamic kinetic activity of PKM2 provides the advantage to response the requirement for fast cell growth in highly proliferating cells such as embryonic and tumor

cells (42). In contrast, PKM1 has a consistent activity and regularly promotes oxidative phosphorylation (OXPHOS) in energy-consuming tissues such as brain and muscle (38, 43).



In cancer cells, the metabolic reconfiguration involves a switch in the expression from PKM1 to PKM2 (44). Furthermore, PKM2 facilitates cellular proliferation by transcriptionally modulating proliferation-associated genes and glycolytic enzymes expression (45). The splicing factors hnRNP A1/A2 and PTB promote PKM2 expression by suppressing PKM exon 9 inclusion. In addition, the oncogenic pathway in cancer cells such as c-Myc can control the expression of these splicing factors to trigger Warburg effect via PKM2 (44).


The PKM isoform switch also correlates with metabolic changes during myoblast and adipocyte differentiation (33, 46). During myoblast differentiation, the reduction of PTB accompanied with the increment of PKM1 splicing isoform (46). In addition, RBM4 modulates the reduction of PKM2 during adipogenic differentiation (33). All these studies suggesting that the splicing switch from PKM2 to PKM1 is crucial for cell differentiation. Nevertheless, whether and how PKM splicing regulated during neuronal differentiation remains largely unknown.



1.5. Regulation of energy metabolism in self-renewal and differentiation of stem cells

Changing metabolic usage between glycolysis and OXPHOS can benefit the cellular requirement and in response to the environment stimuli. For example, producing building blocks including nucleotides and amino acids during rapid cell proliferation required abundant anabolic reactions. In contrast, during cell differentiation, enormous catabolic pathways arise to ensure proper establishment of new cellular functions or to sustain cell homeostasis (47-49).

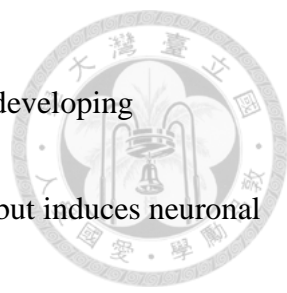
Cellular energy metabolism undergoes a dynamic change during development. The change of metabolism usage can be recapitulated during differentiation of stem cells or the reprogramming of somatic cells into induced pluripotent stem cells (iPSCs) (48-51). In mammals, the glycolysis rate is low in totipotent stem cells (TSCs) at the early embryonic (pre-blastocyst) stage. The carbon source for energy generation mostly relies on pyruvate over glucose at this stage (52, 53). However, the glucose uptake gradually increases at the morula stage, and it increases even more at the blastocyst stage (54). Furthermore, anabolic glycolysis is dominant to lead the lactate production and rapid cell proliferation in embryonic stem cells (ESCs) as well as in cancer cells (48, 49). Upon cell



differentiation, glycolytic flux drops rapidly. Thus, energy pathway switches from glycolysis to OXPHOS (55-57). Interestingly, some studies had indicated that during reprogramming of somatic cells into iPSCs, the energy usage reversed from OXPHOS to glycolysis (58, 59). In addition, most adult stem cells exhibit moderate glycolysis activity in the quiescent state and undertake active glycolysis while proliferating albeit distinct additional metabolism pathways usage upon differentiation (56, 57, 60).

Recently, studies suggested that the metabolic pathway change is not merely a consequence of cell differentiation. Some metabolites function as the post-translational modification substrates such as UDP-GlcAc, which derives from glucose. The UDP-GlcAc can potentially modify stemness factors including OCT4 and SOX2 to maintain the self-renewal function of stem cells (60, 61). Another example is Acetyl-CoA, which is a precursor of acetylation subset proteins involved in energy metabolism or gene expression (48). Moreover, the L-Thr dehydratase (TDH) can increase the synthesis of S-adenosylmethionine (SAM) and further lead to a high level of H3K4me3, which sustaining the pluripotency of ESCs (62).

Besides, the metabolic switch from anabolic glycolysis to OXPHOS is also important for cell cycle exit and cell fate determination. In *Drosophila*, upregulation of OXPHOS is

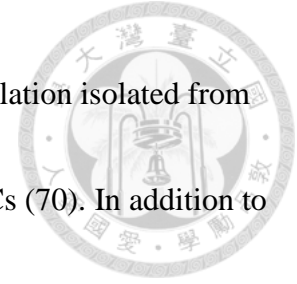


required for terminal differentiation of neural stem cells (63). In the developing mammalian cortex, oxygen tension suppresses radial glia expansion but induces neuronal cell differentiation (64). Analogously, suppression of oxidative metabolism in human glioma resumes neural stem cell proliferation (65). Similarly, maintaining high level of glycolysis by overexpression of hexokinase 2 (HK2) and pyruvate kinase M2 (PKM2) delayed the early differentiation of ECSs (66). Moreover, neurons and astrocytes exhibit distinct metabolic pathways, i.e., OXPHOS and glycolysis, respectively (67). Therefore, metabolic reprogramming influences not only cell cycle progression but also cell specification or terminal differentiation.

Although it is more clear that how AS evens affect the transcription factors expression in stem cells. However, it is remains unclear that whether AS also affect the self-renewal or differentiation of stem cells via regulating cell metabolism.

1.6. Mesenchymal stem cells (MSCs) and its metabolic properties

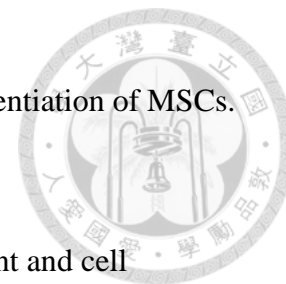
The multipotent stromal precursor cells were first isolated and identified from bone marrow with the potential to differentiate into osteoblasts, chondrocytes, and adipocytes (68). A study further demonstrated the self-renewal and differentiation capacity of these stromal precursor cells and defined it as mesenchymal stem cells (MSCs) (69). Although



MSCs can be isolated from almost every connective tissue, the population isolated from bone marrow was mainly characterized and usually, refer to all MSCs (70). In addition to the ability to differentiate into the cells of mesodermal lineage as identified at initially, MSCs also have the potential in endodermic and neuroectodermic differentiation (71, 72). MSCs have several clinical advantages such as poorly immunogenic and the ability to migrate to inflammation or damage site after injection than other sources of stem cells. Hence, numerous studies focused on the regenerative therapies application of MSCs, including the clinical trials for neurological diseases (73).

Recently, several studies also attended to investigate the metabolism usage of MSCs during differentiation. A study shows that MSCs rely on glycolysis metabolism more than differentiated osteoblast does (56). Intriguingly, the metabolic pathway various among cell types during differentiation of MSCs (49). The usage of OXPHOS is more dominant than glycolysis in osteoblast. Further, both OXPHOS and glycolysis usage increase in pre-adipocytes during adipogenesis. However, the glycolysis is more prevalent than OXPHOS in adipocytes (56, 74). Also, the glycolysis remains major during chondrogenesis from MSCs, and the OXPHOS is lower in chondroblasts than in osteoblasts or pre-adipocytes (49, 75). This dynamic metabolism change during MSCs differentiation can also provide a

chance to investigate the detailed mechanism during neuronal differentiation of MSCs.



Regulation of metabolism usage is critical for organ development and cell differentiation in response to the cellular requirement. The AS events also show the importance for regulating the self-renewal and differentiation of stem cells. However, how AS affects the metabolism change during stem cell differentiation remains largely unclear. Actually, the metabolic change caused by PKM isoform switch is crucial for tumorigenesis and myogenesis. In addition, this isoform switch is regulated by PTB.

Our previous study shown that PKM isoform switch also occurs during neuronal differentiation of P19 cells. The PTB is a major splicing regulator that suppressing neurogenesis. We thus suspect that: 1) PKM isoform switch during neuronal differentiation also regulated by PTB, and, 2) the metabolism change mediated by PKM isoform switch is important for neuronal differentiation. In addition, we had reported that RBM4 modulate myoblast differentiation by suppressing both PTB expression and splicing activity. Thus, we also evaluated whether RBM4 regulate neuronal differentiation by same mechanism.



2. Results

2.1. Pkm isoform switched during mouse embryo development in brain, heart and muscle

PKM1 is expressed in energy-consuming adult tissues, including brain and skeletal muscle, whereas PKM2 is expressed more dominantly in embryonic or cancer cells (45).

We previously observed a change in expression of Pkm isoforms, i.e., from Pkm2 to

Pkm1, during neuronal differentiation of mouse embryonal carcinoma P19 cells (34). I

thus further explored the significance and mechanism of this isoform switch during

development. The precise timing of Pkm isoform switch in mouse tissue is still unclear.

Thus, total RNA isolated from mouse tissues at embryonic day 13.5 (E13.5) to E18.5 were

analyzed by reverse transcription-PCR (RT-PCR) using primers specific to Pkm1 or Pkm2

(Fig. 1A). The results showed a gradual change from Pkm2 to Pkm1 in developing mouse

brain as well as in other tissues, albeit to different extents (Fig. 1B). However, the Pkm2

expression remains dominant even at late embryo stage (E18.5) in pancreas. Thus, Pkm

isoforms expression change only occurs in high energy-consuming tissues during

development.




2.2. RBM4 significantly affects Pkm isoform switch in highly energy-consuming tissues

I found that RBM4 expression levels increased during the period examined in mouse brain from E13.5 to E18.5 (Fig. 2A). Hence, RBM4 may participate in regulating Pkm isoform switch during mouse embryo development. Thus, I examined Pkm isoform expression in RBM4-deficient (i.e. *Rbm4a* or *Rbm4b* knockout) mouse tissues from E13.5 to E18.5. Compared to the levels for wild-type littermates, the level of Pkm2 increased in either *Rbm4* knockout tissues at different development stages (Fig. 2B, E13.5 in brain; Fig. 2C, E18.5 in muscle and heart). Interestingly, the Pkm isoform does not change in RBM4-deficient pancreas (Fig. 2C).

2.3. Mechanisms of RBM4-regulated PKM isoform expression

2.3.1. RBM4 regulates alternative splicing of PKM not by suppressing PTB protein expression

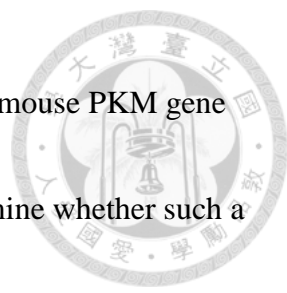
To examine the role of RBM4 in regulating alternative splicing of PKM pre-mRNA, I established a mouse PKM minigene spanning exons 8 to 11 (Fig. 3A). This minigene was cotransfected with a FLAG-RBM4 expression vector into HEK293T cells. The results



showed that the splicing switch from PKM2 to PKM1 correlated with RBM4 expression in a dose-dependent manner (Fig. 3B). PTB is one of the splicing factors, which regulates exon10 splicing in cancer cells or undifferentiated myoblasts (44). Because RBM4 overexpression downregulates PTB expression (Fig. 3C)(31), the argument remained that RBM4 influences PKM splicing merely by suppressing PTB expression. However, I found that a low dose of FLAG-RBM4 (0.05 μ g) did not suppress PTB expression (compare the data for the 0.05- μ g dose in Fig. 3C and D), whereas at this dose or lower doses, RBM4 was sufficient to induce the switch from PKM2 to PKM1 (Fig. 3D). These results suggest that RBM4 regulates PKM splicing directly, not likely through suppression of PTB levels. In addition, when RBM4 and PTB were both overexpressed with the PKM minigene, a high dose of RBM4 could counteract the effect of overexpressed PTB on PKM2 induction (Fig. 3E). Thus, RBM4 also antagonizes the activity of PTB as previously reported (28, 31).

2.3.2. RBM4 regulates alternative splicing of PKM pre-mRNA via an intronic CU-rich sequence

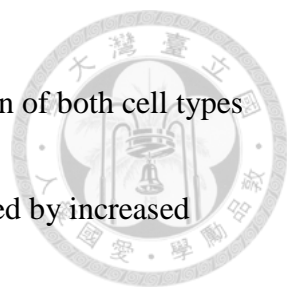
A previous report indicated that PTB suppresses exon 9 usage of human PKM via binding of two UCUU motifs upstream of the 3' splice site of intron 8 (76). RBM4 also



has a preference for CU-rich sequences (28). A CU-rich sequence in mouse PKM gene intron 8 is similar but not identical to its human counterpart. To examine whether such a sequence is responsible for RBM4-mediated splicing regulation, I first performed an electrophoretic mobility shift assay (EMSA). Figure 4A shows that a recombinant maltose binding protein (MBP)-RBM4 fusion bound to the ³²P-labeled CU-rich PKM intron probe but not to the CU-poor control. Next, I generated a CU-rich sequence-truncated minigene. This mutant minigene had a lower capacity for PKM1 expression (Fig. 4B, compare lane 1 and 4). RBM4 was hardly induced PKM1 splicing in the mutant (Fig. 4B), suggesting that RBM4 modulates PKM splicing via binding to the CU-rich sequence in intron 8.

2.4. RBM4 is involved in the PKM isoform switch during neuronal differentiation of human MSCs


Differentiation of human MSCs into osteoblasts involves a metabolic change from glycolysis to OXPHOS (56). I therefore explored whether the PKM isoform switch occurs during MSC differentiation into neuronal cells and whether RBM4 is involved in this process in primary human MSCs and derived 3A6 cells (77). Cells were cultured in neuronal induction medium (NIM) for up to 7 days. The results revealed the change from



PKM2 to PKM1 and an increase in RBM4 level during differentiation of both cell types (Fig. 5A and B). Differentiation of 3A6 cells was further demonstrated by increased expression of several neuron-associated genes, including those encoding neuron-specific class III β -tubulin (TUJ1), microtubule-associated protein 2 (MAP2), synuclein alpha (SNCA), and nuclear receptor subfamily 4 group A member 2 (NR4A2/NURR1), as well as by an increase in the Tuj1 protein level (Fig. 5B).

Next, I assessed whether the RBM4 level affects alternative splicing of PKM in MSCs. I depleted endogenous RBM4 by using a small interfering RNA (siRNA) or transiently overexpressed FLAG-tagged RBM4 in 3A6 cells. Depletion of RBM4 increased PKM2 expression, whereas overexpression of FLAG-RBM4 promoted the production of PKM1 (Fig. 6A). Finally, I performed FLAG-RBM4 immunoprecipitation followed by RT-PCR analysis. The results showed that PKM mRNA was coprecipitated with FLAG-RBM4 in 3A6 cells (Fig. 6B). All these results indicated that RBM4 participates in the PKM splicing switch during neuronal differentiation of MSCs.

2.5. RBM4 promotes neuronal differentiation and neurite outgrowth of MSCs



I assessed whether RBM4 could promote neuronal differentiation of MSCs. Using 3A6 cells, I observed that overexpression of FLAG-RBM4 significantly upregulated the expression of neuronal genes in noninduced cells (Fig. 7A). In contrast, the expression of two stemness genes, OCT4 and SOX2, and one proliferation-related gene, HES1, was downregulated by RBM4 (Fig. 7A). Next, I depleted RBM4 in 3A6 cells cultured under differentiation conditions. RBM4-deficient cells exhibited delayed or reduced expression of the neuronal markers TUJ1 and MAP2 (Fig. 7B). These results indicate the expression of RBM4 is required for neuronal differentiation of MSCs.

Finally, I examined cell morphologic changes of RBM4-overexpressing cells. I observed only a small proportion of RBM4-overexpressing 3A6 cells that could generate neurites under noninduced conditions (Fig. 8A). Nevertheless, when cells were cultured under differentiation conditions, I observed that RBM4 overexpression considerably promoted neurite outgrowth by immunofluorescence staining for Tuj1 (Fig. 8B). These results further suggested that RBM4 plays an important, though not initiating, role in promoting neuronal differentiation.

2.6. RBM4-regulated PKM1 isoform expression enhances mitochondrial OXPHOS and promotes neuronal differentiation of MSCs



During cell differentiation, the energy usage changed from glycolysis to OXPHOS (55-57). In addition, the mitochondrial bioenergetics and function are upregulated during neuronal differentiation (78). Thus, I assessed whether RBM4 and PKM1 could also trigger the change in energy generation from glycolysis to OXPHOS during neuronal differentiation. I used the Seahorse XF analysis system to evaluate the oxygen consumption rate (OCR) in noninduced 3A6 cells. Overexpression of RBM4 or PKM1 resulted in a ~30% higher basal oxygen consumption rate and maximal respiration than those of the control (Fig. 9). In contrast, PKM2 significantly reduced ATP production, by ~50% (Fig. 9). This observation suggested that RBM4-induced PKM1 is important for altering energy metabolism during neuronal differentiation of MSCs.

The above result that the relative level of PKM1 increased gradually during MSC neuronal differentiation (Fig. 5) and was elevated by RBM4 overexpression (Fig. 6A) suggesting that PKM1 also promotes neuronal differentiation. I found that overexpression of PKM1 upregulated the expression of both the TUJ1 and MAP2 genes in noninduced MSCs (Fig. 10A). Immunoblotting confirmed Tuj1 protein expression also induced by



PKM1 but not PKM2 (Fig. 10A). Furthermore, I overexpressed PKM1 in RBM4-depletion 3A6 cells, and observed that PKM1 was able to restore neuronal gene expression and to suppress negative regulators in the absence of RBM4 (Fig. 10B).

Moreover, PKM1 enhanced neurite outgrowth under differentiation conditions, as observed with RBM4 (Fig. 11). Unlike RBM4 or PKM1, the PKM2 negatively affected neuronal gene expression and neurite outgrowth (Fig. 10A and Fig. 11, 24 h). This result strengthened the role of PKM1 in neuronal differentiation.

PKM2 facilitates cellular proliferation by transcriptionally modulating proliferation-associated genes and glycolytic enzymes expression (45). Thus, the isoforms switch from PKM2 to PKM1 during neuronal differentiation of MSCs may also affect the glycolytic enzymes expression and even lower cell proliferation rate. The expression change between lactate dehydrogenase A (LDHA) and LDHB was correlated with energy metabolic state.

LDHA is dominantly expressed under anabolic glycolysis. The RT-PCR result shows that PKM1 enhanced LDH1 expression, however, PKM2 promotes LDHA (Fig 12A).

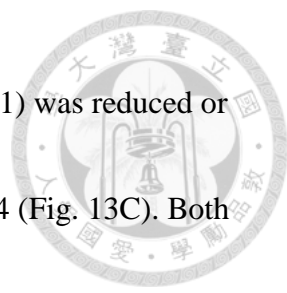
Overexpression of RBM4 shows a similar result with PKM1 although HK1 does not change significantly (Fig 12A, B). I also examined the cellular growth by overexpression RBM4, PKM1 or PKM2 respectively. The result shows that RBM4 and PKM1

overexpression cells slightly reduced the cell growth rate compared to control or PKM2 overexpression cells (Fig. 12C). The above results suggested that the differential expression of PKM isoforms affect the metabolic related enzyme such as LDH expression and also cell proliferation.



2.7. RBM4 promotes neuronal differentiation via suppressing a negative regulating pathway

The data consistently showed that RBM4 had higher capacity than that of PKM1 to promote neurite outgrowth at later postinduction time points (24h)(Fig. 11). Perhaps RBM4 promotes the expression of a wider range of neuronal genes than that promoted by PKM1. To further evaluate the role of RBM4 in neuronal differentiation and neurite outgrowth, I took advantage of a quantitative PCR-array analysis in RBM4-overexpressing 3A6 cells with or without NIM treatment (24h). I observed that the expression of several genes was affected by overexpression of RBM4, which involved in different aspect of neurogenesis including Notch or bone morphogenetic protein (BMP) signaling, or synaptic functions (Fig. 13A). I further confirmed that the level of BMP2 was reproducibly downregulated in several independent experiments (Fig. 13B). Accordingly, the expression



of the BMP2 downstream target DNA-binding protein inhibitor 1 (Id1) was reduced or increased upon overexpression or knockdown, respectively, of RBM4 (Fig. 13C). Both BMP2 and Id1 have negative roles in neuronal differentiation (79). Therefore, RBM4 may downregulate the BMP-Id1 pathway to promote neuronal differentiation of MSCs.

2.8. Hypoxia environment induces RBM4 expression and neuronal differentiation of MSCs

It has been reported that hypoxic conditions or expression of hypoxia-inducible factor 1a (HIF-1a) can promote neuronal differentiation of MSCs (80, 81). Therefore, I cultured noninduced 3A6 cells at 1% oxygen or in the presence of the hypoxia-mimetic agent cobalt chloride (CoCl₂) (Fig. 14A). Low oxygen triggered HIF-1a expression, as expected, and increased the levels of neuronal markers (TUJ1 and MAP2 mRNAs) and the RBM4 protein (Fig. 14A). This result indicated that hypoxia was sufficient to initiate neuronal differentiation. Moreover, the increase in RBM4 prompted us to examine whether HIF-1a could induce the expression of RBM4. I transiently overexpressed hemagglutinin (HA)-tagged HIF-1a in 3A6 cells and observed an increase in both RBM4A and RBM4B mRNAs as well as RBM4 protein (Fig. 14B), suggesting that HIF-1a regulates RBM4

expression through transcriptional control. CoCl₂ also induced the expression of HIF-1α and RBM4 proteins (Fig. 14A, IB panels) as well as TUJ1 and MAP2 mRNAs, consistent with the results from the low-oxygen experiment.



2.9. RBM4 is involved in the hypoxia-induced switch of PKM splice isoforms and neuronal differentiation

I examined PKM isoform expression in CoCl₂-treated 3A6 cells. It has been reported that PKM expression can be induced by HIF-1α (82). Regardless of increased total PKM levels, the ratio of PKM1 to PKM2 was still increased upon CoCl₂ treatment, coordinately with the increase in RBM4 (Fig. 14A and Fig. 15A). Next, I depleted RBM4 by use of siRNA in CoCl₂-treated 3A6 cells and observed that both the induction of MAP2 and the PKM2-to-PKM1 switch were abolished (Fig. 15B). However, the increase of overall PKM expression was unaffected. This result indicated that RBM4 is essential for hypoxia-induced neuronal differentiation and the PKM isoform switch.



2.10. RBM4 induces the expression of a PTB isoform with attenuated splicing activity in human MSCs

RBM4 promotes the expression of the exon 11-skipping PTB mRNA isoform and thereby downregulates PTB expression via nonsense-mediated mRNA decay (NMD) in various cell types (31, 33). I wondered whether RBM4 also reduces PTB expression during neuronal differentiation of MSCs. In 3A6 cells, exon 11 skipping of PTB mRNA was not readily detected even in the presence of cycloheximide (CHX) and was induced very minimally by RBM4 overexpression, unlike observations in mouse myoblast C2C12 cells (Fig. 16A, data for PTB-4^{-e11} and PTB-1^{-e11}). Nevertheless, the observation that RBM4 overexpression slightly induced exon 9 skipping of PTB in 3A6 cells (Fig. 16A, lane 2) was reminiscent of a recent report that the exon 9-skipping isoform of PTB (PTB-1) is induced during neuronal differentiation of mouse embryonic stem cells (83). I indeed observed that exon 9 skipping of PTB increased gradually during neuronal differentiation of primary MSCs (Fig. 16B, RT-PCR panel). Immunoblotting with anti-PTB confirmed the change from the exon 9-containing to the exon 9-skipping isoform (Fig. 16B, IB panel). RBM4-induced exon 9 skipping was observed in 3A6 cells and, even more robustly, in HeLa and HEK293T cells (Fig. 16C, RT-PCR panels). Accordingly, RBM4

overexpression raised the PTB-1 protein level, albeit minimally (Fig. 16C, IB panels).

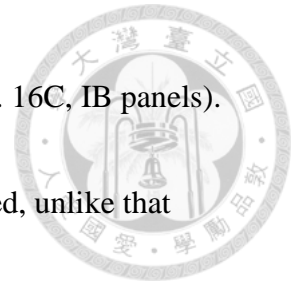
Under these conditions, the overall PTB protein level was not reduced, unlike that

observed in other cell types (Fig. 3)(31, 33). With all these data, I provide evidence that

RBM4 induces a PTB protein isoform, PTB-1, in MSCs without affecting the overall PTB level.

Next, I generated a PTB minigene spanning exons 8 to 10 and performed an *in vivo* splicing assay in both 3A6 and HEK293T cells. The result confirmed the activity of RBM4 in promoting exon 9 skipping (Fig. 16D). Immunoprecipitation and RT-PCR demonstrated the association of FLAG-RBM4 with endogenous PTB transcripts in 3A6 cells (Fig. 16E), emphasizing the direct role of RBM4 in the splicing or biogenesis of PTB transcripts.

Finally, I assessed whether PTB-1 and PTB-4 exhibit different activities in PKM splicing. Using the minigene assay, I observed that both isoforms could reduce the ratio of PKM1 to total PKM (Fig. 18A). PTB-4 appeared to have a higher activity than that of PTB-1, as recently reported (83). Interestingly, loss of PTB-4 (but not PTB-1) by using the shPTB clone shows PTB-1 has a weaker activity to induce PKM2 splicing, which similar to minigene assay (Fig. 18A and B, RT-PCR panel). In addition, the result



shows that overexpression of PTB-1 induced neuronal markers expression and suppressed BMP-2 pathway as RBM4 (Fig. 13 and Fig. 17C). The above results suggesting that the isoform change from PTB-4 to PTB-1 by RBM4 also involved in neuronal differentiation of MSCs.



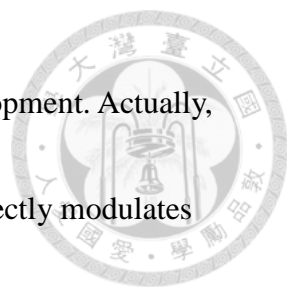
3. Discussion

3.1. RBM4 directly modulates PKM isoform switch in the developing brain



The isoform switch from Pkm2 to Pkm1 during myoblast differentiation has been reported before (46). However, the exact timing and the regulatory mechanism during development in the embryonic mouse are remained unclear. In this study, I observed a gradual Pkm isoform switch toward Pkm1 in mouse brain, heart, and muscle, but not in pancreas during embryonic development (Fig. 1). This observation is consistent with a report that the expression of PKM1 over PKM2 restricts in adult energy-consumption tissue in human (44). I also found an isoform switch toward PKM1 under the neuronal induction condition of MSCs (Fig. 5). Thus, this splicing switch event in specific tissues might be critical because of the conservation between human and mouse.

A study identified that three splicing factors, including hnRNPA1/A2 and PTB, regulate PKM2 splicing in cancer cells (44). The PTB is an important splicing regulator that suppress neuronal differentiation via regulating subset AS events (20). We previous demonstrated that RBM4 regulates PTB expression during myogenesis (31). Moreover, the Human Protein Atlas database showing that RBM4 expression is enriched in the brain, especially in neurons. Thus, it is reasonable that, RBM4, the upstream regulator of PTB,




could also affect the AS of PKM during neurogenesis or brain development. Actually, RBM4 not only antagonizes the splicing activity of PTB but also directly modulates PKM1 splicing via an interaction with the CU-rich sequences on PKM gene intron 8, without suppressing the PTB level (Fig. 3, 4). These results can explain the aberrant splicing of PKM in the RBM4 deficient mouse tissues (Fig. 2) and suggest that RBM4 is an important regulator in modulating the AS of PKM pre-mRNA.

3.2. The RBM4-mediated PKM isoform shift contributes to neuronal differentiation.

A significant metabolic utilize shift from anabolic glycolysis to OXPHOS is occurs during cell differentiation in ESCs (57). Although the mechanism that PKM2 mediates anabolic glycolysis in cancer cells is extensively characterized (45), whether the PKM1 expression is critical or not to tissue development still largely unknown. In this study, the prominent Pkm2-to-Pkm1 switch in the embryonic brain echoes the metabolic shift from glycolysis to OXPHOS during neurogenesis (Fig. 1)(63, 64). These results suggest that PKM isoform switch mediates the metabolic shift in differentiating cells as cancer cells, albeit in a reverse direction.

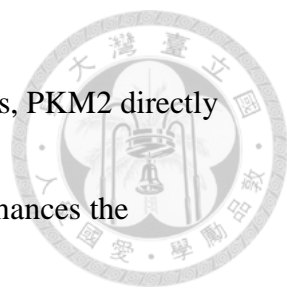
MSCs have a potential to differentiate into various cell types that display distinct



metabolic properties (49). In this study, I observed that the PKM splice isoform change occurs in both primary MSCs and 3A6 cells (Fig. 5). I also noted that both RBM4 and PKM1 significantly elevate the OXPHOS utilization, whereas PKM2 greatly reduces the ATP production of MSCs (Fig. 9). These results demonstrate that RBM4-mediated PKM isoform switch indeed changes the metabolism pathway usage of MSCs.

Furthermore, my result showing that PKM1 can upregulate neuronal markers and enhance neurite outgrowth (Fig. 10, 11) argues that the splicing change of PKM is not merely a consequence of cell differentiation. A recent report indicated that mitochondrial bioenergetics and function are upregulated during neuronal differentiation (78). Moreover, fine-tuning of metabolic regulation is critical for the function and cell fate decisions of neural stem/progenitor cells (63-67), emphasizing the role of the PKM splicing switch in neurogenesis. My results reveal, for the first time, the significance of the RBM4-PKM1 pathway in neuronal differentiation and possibly also in brain development, by enhancing mitochondrial respiratory capacity.

In cancer cells, PKM2 not only contributes to intricate metabolic reprogramming but also acts as a transcriptional activator (45). The translocation of PKM2 from cytosol to nuclear promotes several glycolytic enzymes expression such as pyruvate dehydrogenase



kinase-1 (PDK-1), and lactate dehydrogenase (LDH)(78, 82). Besides, PKM2 directly interacts with octamer-binding transcription factor 4 (OCT4) and enhances the transcriptional activity of OCT4, a transcription factor that maintains stemness of undifferentiated stem cells (84). Moreover, PKM2 participate in the epigenetic regulation of phosphorylation of histone H3, via its protein kinase activity (85). Thus, the splicing switch from PKM2 to PKM1 during neuronal differentiation may not merely lead a metabolism pathway shift. Indeed, I observed a slight reduction of cell growth in RBM4 and PKM1 overexpression MSCs (Fig. 12). Moreover, the PKM1 and PKM2 induce different glycolytic enzymes expression, including LDHA and LDHB of MSCs (Fig. 12). Thus, the reduced level of PKM2 in developing embryonic mouse brains and differentiating primary MSCs may result in an extension of cell proliferation or a reduction of the stemness ability of stem cells. However, the unapparent effect of cell proliferation or glycolytic genes expression may lead due to the remaining endogenous PKM level (i.e. overexpression PKM1 did not reduce PKM2 expression). Nevertheless, my results still provide some additional roles that how PKM isoform shift enhances neuronal differentiation of MSCs.



3.3. RBM4 regulates neuronal differentiation and neuronal function via various pathways

PKM1 directly promotes neuronal differentiation of MSCs, and it is able to restore neuronal gene expression and to suppress negative regulators in the absence of RBM4 (Fig. 10). However, this study also shows that RBM4 has a higher capacity than that of PKM1 to promote neurite outgrowth at later postinduction time points (24h)(Fig.11). In addition, my qPCR array results show that RBM4 upregulates several genes expression involving in synaptogenesis or synaptic functions (Fig. 13). Thus, RBM4 may modulate distinct pathways throughout neuronal differentiation: RBM4-PKM isoform shift promotes the early differentiation, then, enhances the maturation of neuron by activating gene expression involved in synaptogenesis.

Intriguingly, neurons and astrocytes exhibit distinct metabolic pathways, i.e., OXPHOS and glycolysis, respectively, according to their functions (67). A study showed that the gradual expression difference of metabolic enzymes such as PKM1 (in neurons) and PKM2 (in astrocytes) exist in these two lineages (86). Therefore, the RBM4-mediated PKM isoform switch may not only promote differentiation but also sustain the cellular functions in mature neurons. In addition, our lab also characterized a role of RBM4 in

regulating neuron migration via Dab1 pathway (unpublished data). Thus, RBM4 may participate in many processes during brain development. However, the detailed mechanism still needs to be elucidated.



3.4. Hypoxia induces neuronal differentiation via the RBM4-mediated PKM isoform shift

MSCs reside in natural niches, in which the concentration of oxygen ranges from 1 to 6%. A hypoxic environment is critical for MSCs to maintain both the potential for self-renewal and plasticity (87). Nonetheless, it has been reported that hypoxic treatment can promote neuronal differentiation of various stem cells (88). The activated p38 or ERK pathway could upregulate HIF-1a expression of MSCs during hypoxia-induced neuronal differentiation (80). In addition, HIF-1a promotes neuronal differentiation of MSCs by provoking cell cycle arrest (89). I showed that hypoxic treatment induced neuronal gene expression concurrent with an increase in HIF-1a supporting the idea that hypoxia enhances the potential for neuronal differentiation (Fig. 14). Moreover, I observed that HIF-1a induced RBM4 expression at the transcriptional level and demonstrated that RBM4 is essential for the hypoxia-induced PKM isoform switch as well as neuronal gene

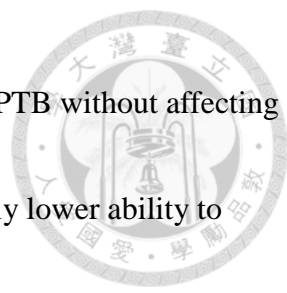
expression (Fig. 15). A computational search revealed potential HIF-1 α /ARNT binding motifs in the promoters of both the RBM4A and RBM4B genes



(http://jaspar.genereg.net/cgi-bin/jaspar_db.pl). Thus, HIF-1 α -induced RBM4 expression also provides a hint as to the function of RBM4 in other physiological and pathological low-oxygen conditions.

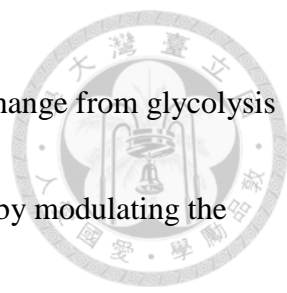
3.5. RBM4 regulates PTB isoform expression and suppresses PTB activity in MSCs

The splicing factors hnRNP A1/A2 and PTB regulate PKM pre-mRNA splicing by suppressing exon 9 selection (76), in a manner opposite to that of RBM4 (Fig. 3, 4). PTB regulates a set of alternative splicing events that suppress neuronal differentiation in non-neuronal cells (20). In addition, PTB expression can be post-transcriptionally regulated by microRNAs or through alternative splicing-coupled NMD during neuronal differentiation (20, 90). Actually, exon 11-skipped PTB is the NMD-susceptible isoform. Studies had shown that RBM4 downregulates PTB expression during myogenesis and adipogenesis by promoting exon 11 skipping (31, 33). Nevertheless, neither RBM4-induced exon 11 skipping nor cycloheximide-stabilized PTB transcripts were significantly detected in MSCs (Fig. 16). Perhaps NMD activity was compromised during stem cell differentiation



(91). Instead, RBM4 could induce the expression of exon 9-skipped PTB without affecting overall PTB protein expression in MSCs. This isoform has a relatively lower ability to suppress alternative exons of neuronal transcripts during stem cell differentiation into neurons (Fig. 17) (83). Moreover, RBM4 antagonized the activity of PTB in splicing regulation (Fig. 3). Thus, my finding adds to the known repertoire of RBM4 functions in modulating PTB expression and activity. Perhaps it is necessary to maintain a low level of PTB activity at early stages of stem cell differentiation. While neuronal cell fate is determined, PTB may be subsequently and completely suppressed by microRNAs (90). Together, our past and present results demonstrate that RBM4 suppresses PTB activity via multiple pathways (Fig. 18). RBM4 may fine tune mRNA isoform expression by inducing a less-active PTB isoform as well as antagonizing the activity or function of PTB in stem cells. Finally, the result that PTB promotes PKM2 expression provides a hint that PTB acts as a negative regulator of neuronal differentiation. In fact, knockdown of PTB increased the expression neuronal markers and reduced the expression of the BMP pathway (Fig. 17). Thus, RBM4 and PTB may function oppositely in neuronal differentiation.

In this dissertation, I use MSCs as a cellular model to explore the detailed mechanism



of neuronal differentiation, which accompanied with a metabolism change from glycolysis to OXPHOS. I have demonstrated that RBM4 regulates this process by modulating the splicing switch of PKM1 and PKM2. In addition, RBM4-modulated PKM1 expression enhanced the metabolic usage toward to OXPHOS of MSCs. I further found that PKM1 directly induces neuronal differentiation as RBM4. Thus, the metabolic change via RBM4-PKM1 axis is not merely a consequence of cellular differentiation. Interestingly, RBM4 also had been reported that it suppresses tumor progression. Moreover, PKM2 is required for tumorigenesis via leading the Warburg effect. Thus, it is possible that RBM4 suppresses tumor progression via changing the alternative splicing of PKM isoforms.

Besides, I also observed that the HIF-1 α -RBM4-PKM axis enhances the neuronal differentiation of MSCs under a hypoxia condition. This finding reveals new and biologically important targets of RBM4 and provides a potential for RBM4-mediated neuronal differentiation of MSCs in therapies for neurodegenerative diseases.

Finally, I uncovered a distinct regulation mechanism of PTB, which modulated by RBM4 in a cell-specific manner. The PTB is a master splicing regulator for modulating neurogenesis. RBM4 is also important to regulate neuronal differentiation at least by regulating alternative splicing of NUMB, PKM, and PTB. Thus, during neuronal

differentiation, whether RBM4 also modulates the common set of alternative splicing targets with PTB as in myoblast differentiation is still need to investigate.





4. Materials and methods

Animals and ethics statement

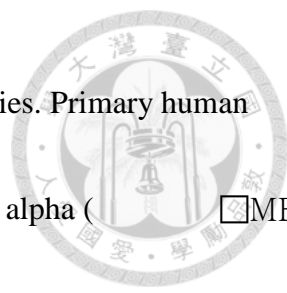
This study was approved by the Institutional Animal Care and Use Committee (IACUC) of Academia Sinica and was compliant with the Taiwan Ministry of Science and Technology guidelines for ethical treatment of animals. Mice were housed and handled under the guidelines of IACUC.

Embryonic mouse tissues isolation and RT-PCR

Rbm4a and *Rbm4b* knockout mice have been described (32). Embryonic mouse brain, heart, muscle and pancreas were isolated at embryonic day (E) 13.5, 15.5 and 18.5. The brain of *Rbm4* knockout or wild-type embryos was isolated at embryonic day 13.5. Total RNA was extracted by using TRIzol reagent (Thermo Fisher Scientific) following the instructions. For reverse-transcription (RT), 2 µg of extracted RNA was treated with RQ1 DNase (Promega) and followed by using SuperScript III kit (Life Technologies). PCR primer sets were listed in Supplemental Table S1.

Cell culture, neuronal differentiation and hypoxic induction

Human primary mesenchymal stem cells (MSCs) and derived line 3A6 cells have been previously described (77). 3A6 cells immortalized by HPV16 E6E7 ectopically express



human telomerase reverse transcriptase to gain stem cell-like properties. Primary human MSCs and 3A6 cells were maintained the Minimum Essential Media alpha (MEM, Gibco) and low-glucose Dulbecco's Modified Eagle's Medium (LG-DMEM, Gibco), respectively. C2C12 myoblast, HeLa cells and HEK293T cells were cultured in DMEM (Gibco) with the same supplement. All above mediums were supplemented with 10% fetal bovine serum (Gibco), 100 U/ml penicillin and 100 µg/ml streptomycin (Life Technologies). All cells were cultured in 37°C humidified incubators with 5% CO₂. For neuronal differentiation, primary MSCs or 3A6 cells were seeded at a density of 4,000 cells/cm² and induced by neuronal induction medium (NIM) containing DMEM without serum and supplement with 0.1 µM dexamethasone (Sigma), 50 µg/mL ascorbic acid-2 phosphate (Sigma), 50 µM indomethacin (Sigma), and 10 µg/mL insulin (Sigma) in the next day (77). The medium was changed every three days. For hypoxic induction, 3A6 cells were incubated in 1% O₂ incubator or treated with 200 µM CoCl₂ up to 24 hrs.

Immunoblotting and indirect immunofluorescence

Immunoblotting was performed using enhanced chemiluminescence system (Millipore) as described (26). Primary antibodies used included polyclonal antibodies against RBM4 (31), α -Tubulin (NeoMarkers), FLAG tag (Sigma-Aldrich), Tuj1 (Biolegend), PTB

(Abcam) and HIF-1a (Proteintech). For indirect immunofluorescence, transfected cells were induced in NIM for 0, 5 or 24 hrs and sequentially treated with 3% formaldehyde (Merck) and 0.5% Triton X-100 (Sigma). The fluorescence staining was performed as described (26). The image was observed by using Laser Scanning Microscope (LSM 700, Zeiss).

Plasmid construction

The expression vectors of FLAG-tagged RBM4 and PTB were described previously (31). To generate the expression vectors of FLAG-tagged PKM1, PKM2, I performed RT-PCR using 3A6 cell total RNA with specific primers and cloned each cDNA into the pcDNA3.1 vector. To construct the mouse PKM minigene reporter, three genomic DNA fragments, including one from exon 8 to the 5' part of intron 8, one from 3' part of intron 8 to 5' part of intron 10 and one from 3' part of intron 10 to exon 11, were amplified and ligated and the resulting DNA was cloned into pCH110 (GE Healthcare). The mutant PKM reporter was generated by PCR-based mutagenesis. To construct the human PTB minigene, two genomic DNA fragments, one from exon 8 to the 5' part of intron 9 and the other from the 3' part of intron 9 to exon 10, were amplified and ligated and the resulting DNA was subcloned into pCH110. To construct the FLAG-PTB-1 and PTB-4 expression vectors,



RT-PCR was performed using 3A6 cell cDNA as template and one set of primers (Supplemental Table S1). The corresponding cDNAs were each subcloned into a FLAG-containing pCDNA3.1. The expression vector of HA-tagged HIF-1a was from Y.-S. Huang (Academia Sinica, Taipei).

Transfection, *in vivo* splicing assay and cycloheximide treatment

C2C12 myoblast, HeLa cells and HEK293T cells were grown to 80% confluency in each 6 well plate and transfected by using Lipofectamine 2000 (Life Technologies). For 3A6 cells, 2×10^5 cells were seeded in 6 well plates and transfected using GenJet in vitro DNA transfection reagent (Version II) (SignaGen). In general, 0.5 μg of the reporter was co-transfected with indicated amounts of the splicing effectors into HEK293 cells for 30 h. Total RNA was isolated for RT-PCR analysis using specific primers (Supplemental Table S1). To enhance the PCR signals, Southern blotting was performed using specific primers (Supplemental Table S1, [31]). For cycloheximide (CHX) treatment, cells were transfected with the RBM4 expression vector or empty vector for 30 hrs. The cells were treated with or without CHX for 2 hrs before harvest. For knockdown specific gene expression, 20 pmol of siRNA (Stealth siRNA, Invitrogen) were used to target luciferase (siLuc) or RBM4 (siRBM4) (sense GCGUACGCCUUACACCAUGAGUUAU and

antisense AUAACUCAUGGUGUAAGGCGUACGC).



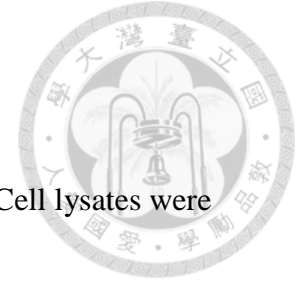
Cell metabolism assay

3A6 cells were transfected with a FLAG-protein (RBM4, PKM1 or PKM2) expression vector or an empty vector for 30 h. For oxygen consumption rate (OCR) analysis, I exploited the Seahorse system (Agilent Technologies). In brief, 1×10^4 transfected cells were seeded in Seahorse XF 98 plates for 24 hrs and the medium was changed 1 hr before analysis. Analysis was performed according to the manufacturer's instruction. To gain a complete mitochondrial profile, I used the Mito Stress Test kit (Agilent Technologies) and followed the instruction sequentially adding oligomycin (1 μ M), FCCP (1 μ M) and Rotenone/Antimycin (0.5 μ M).

RT-PCR and RT-qPCR assay

Reverse transcription-PCR was performed essentially as described previously (31).

Primers used are listed in Supplemental Table S1. To search for potential RBM4 targets during neuronal differentiation of MSCs, I used Neurogenesis qPCR Array (PAHS-404Z, QIAGEN). 3A6 cells were transfected with the FLAG-RBM4 or empty vector for 30 hrs. Cells were re-seeded at a density of 4,000 cells/cm² and cultured in NIM for 1 day. Total RNA was extracted for analysis according to the manufacturer's instruction.



RNP immunoprecipitation

The FLAG-RBM4 vector was transfected into 3A6 cells for 30 hrs. Cell lysates were prepared and incubated with anti-FLAG M2 beads (Sigma) in the NET-2 buffer (50 mM Tris-HCl, pH 7.4, 150 mM NaCl and 0.1% NP-40) at 4°C for 2 h. After extensive washing with NET-2, RNA was extracted by using the TRIzol reagent. RT-PCR was performed using primers in Supplementary Table S1.

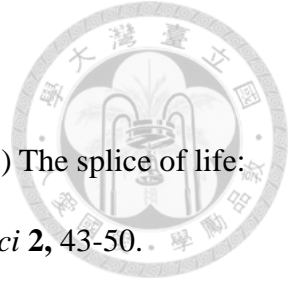
Electrophoretic mobility shift assay (EMSA)

The CU-rich RNA probe contained a 61-nt fragment derived from the 3' end of mouse PKM intron 8 (i.e. 7 to 67 nt upstream of the 3' splice site). The control contained a 45-nt CU-poor sequence, 393 to 437 nt upstream of the 3' splice site. The probe cDNAs were each subcloned into pGEMT vector (Promega). The RNA probes were *in vitro* transcribed from NotI-linearized plasmids by using T7 RNA polymerase (Promega). EMSA was performed essentially as described (31). Recombinant maltose binding protein (MBP) and MBP-RBM4 proteins were previously described (31). For RNA-protein interaction, 2.8 μg (~55 pmol) of recombinant MBP-RBM4 was incubated with 5×10^4 cpm of ^{32}P -labeled probe (75 fmol for the CU-rich probe) at 30°C for 30 min. The reactions were analyzed by electrophoresis on a 6% nondenaturing polyacrylamide gel as described (31).

Statistical analysis

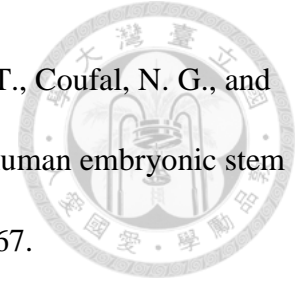
The Student's t-test was performed to evaluate significant difference between experimental groups. Error bars in all graphs indicated standard errors of the mean. The p -values <0.05 was considered statistically significant.



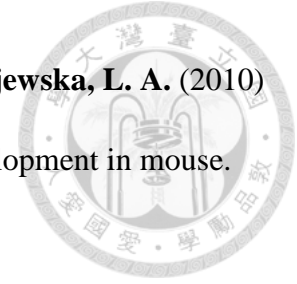


Reference

1. **Dredge, B. K., Polydorides, A. D., and Damell, R. B.** (2001) The splice of life: alternative splicing and neurological disease. *Nat Rev Neurosci* **2**, 43-50.
2. **Matlin, A. J., Clark, F., and Smith, C. W.** (2005) Understanding alternative splicing: towards a cellular code. *Nat Rev Mol Cell Biol* **6**, 386-398.
3. **Will, C. L., and Lührmann, R.** (2011) Spliceosome structure and function. *Cold Spring Harb Perspect Biol* **3**, a003707.
4. **Matera, A.G., and Wang, Z.** (2014) A day in the life of the spliceosome. *Nat. Rev. Mol Cell Biol* **15**, 108-121.
5. **Fu, X. D., and Ares, M.** (2014) Context-dependent control of alternative splicing by RNA-binding proteins. *Nat Rev Genet* **15**, 689-701.
6. **Lee, Y., and Rio, D. C.** (2015) Mechanisms and regulation of alternative pre-mRNA splicing. *Annu Rev Biochem* **84**, 291-323.
7. **Salomonis, N., Schlieve, C. R., Pereira, L., Wahlquist, C., Colas, A., Zambon, A. C., Vranizan, K., Spindler, M. J., Picoo, A. R., Cline, M. S., Clark, T. A., Williams, A., Blume, J. E., Samal, E., Mercola, M., Merrill, B. J., and Conklin, B. R.** (2010) Alternative splicing regulates mouse embryonic stem cell pluripotency and differentiation. *Proc Natl Acad Sci U S A* **107**, 10514-10519.
8. **Pritsker, M., Doniger, T. T., Kramer, L. C., Westcot, S. E., and Lemischka, I. R.** (2005) Diversification of stem cell molecular repertoire by alternative splicing. *Proc Natl Acad Sci U S A* **102**, 14290-14295.
9. **Atlasi, Y., Mowla, S. J., Ziaee, S. A., Gokhale, P. J., and Andrews, P. W.** (2008) OCT4 spliced variants are differentially expressed in human pluripotent and nonpluripotent cells. *Stem Cells* **26**, 3068-3074.



10. Yeo, G. W., Xu, X., Liang, T. Y., Muotri, A. R., Carson, C. T., Coufal, N. G., and Gage, F. H. (2007) Alternative splicing events identified in human embryonic stem cells and neural progenitors. *PLoS Comput. Biol.* **3**, 1951-1967.
11. Chen, X., Xu, H., Yuan, P., Fang, F., Huss, M., Vega, V. B., Wong, E., Orlov, Y. L., Zhang, W., Jiang, J., Loh, Y. H., Yeo, H. C., Yeo, Z. X., Narang, V., Govindarajan, K. R., Leong, B., Shahab, A., Ruan, Y., Bourque, G., Sung, W. K., Charke, N. D., Wei, C. L., and Ng, H. H. (2008) Integration of external signaling pathways with the core transcriptional network in embryonic stem cells. *Cell* **133**, 1106-1117.
12. Kim, J., Chu, J., Shen, X., Wang, J., and Orkin, S. H. (2008) An extended transcriptional network for pluripotency of embryonic stem cells. *Cell* **132**, 1049-1061.
13. Wang, B., Weidenfeld, J., Lu, M.M., Maika, S., Kuziel, W.A., Morrissey, E.E., and Tucker, P.W. (2004) Foxp1 regulates cardiac outflow tract, endocardial cushion morphogenesis and myocyte proliferation and maturation. *Development* **131**, 4477-4487.
14. Gabut, M., Samavarchi-Teheani, P., Wang, X., Slobodeniuc, V., O'Hanlon, D., Sung, H. K., Alvarez, M., Talukder, S., Pan, Q., Mazzoni, E. O., Nedelec, S., Wichterle, H., Woltjen, K., Hughes, T. R., Zandstra, P. W., Nagy, A., Wrana, J. L., and Blencowe, B. J. (2011) An alternative splicing switch regulates embryonic stem cell pluripotency and reprogramming. *Cell* **147**, 132-146.



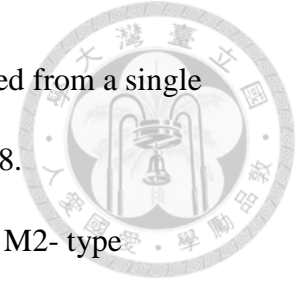
15. **Revil T, Gaffney D, Dias C, Majewski J, and Jerome-Majewska, L. A.** (2010) Alternative splicing is frequent during early embryonic development in mouse. *BMC Genomics* **11**, 399.
16. **Barbosa-Morais, N. L., Irimia, M., Pan, Q., Xiong, H.Y., Guerousov, S., Lee, L. J., Slobodeniuc, V., Kutter, C., Watt, S., Çolak, R., Kim, T., MisquittapAli, C. M., Wilson, M. D., Kim, P. M., Odom, D. T., Frey, B. J., and Blencowe, B. J.** (2012) The evolutionary landscape of alternative splicing in vertebrate species. *Science* **338**, 1587–1593.
17. **Merkin, J., Russell, C., Chen, P., and Burge, C.B.** (2012) Evolutionary dynamics of gene and isoform regulation in Mammalian tissues. *Science* **338**, 1593–1599.
18. **Rai, B., and Blencowe, B. J.** (2015) Alternative Splicing in the Mammalian Nervous System: Recent Insights into Mechanisms and Functional Roles. *Neuron* **87**, 14-27.
19. **Vuong, C. K., Black, D. L, and Zheng, S.** (2016) The neurogenetics of alternative splicing. *Nat Rev* **17**, 265-281.
20. **Boutz, P. L., Stoilov, P., Li, Q., Lin, C. H., Chawla, G., Ostrow, K., Shiue, L., Ares, M. Jr., and Black, D. L.** (2007) A post-transcriptional regulatory switch in polypyrimidine tract-binding proteins reprograms alternative splicing in developing neurons. *Genes Dev* **21**, 1636-1652.
21. **Rai, B., O’Hanlon, D., Vessey, J. P., Pan, Q., Ray, D., Buckley, N. J., Miller, F. D. and Blencowe, B. J.** (2011) Cross-regulation between an alternative splicing activator and a transcription repressor control neurogenesis. *Mol Cell* **43**, 843-850.
22. **Gehman, L. T., Stoilov, P., Maguire, J., Damianov, A., Lin, C. H., Shiue, L.,**



- Ares, M. Jr., Mody, I., and Black, D. L. (2011) The splicing regulator Rbfox1 (A2BP1) control neuronal excitation in the mammalian brain. *Nat Genet* **43**, 706-711.
23. Gehman, L. T., Meera, P., Stoilov, P., Shiue, L., O'Brien, J. E., Meisler, M. H., Ares, M. Jr., Otis, T. S., and Black, D. L. (2012) The splicing regulator Rbfox2 is required for both cerebellar development and mature motor function. *Genes Dev* **26**, 445-460.
24. Jensen, K. B., Dredge, B. K., Stefani, G., Zhong, R., Buckanovich, R. J., Okano, H. J., Yang, Y. Y., and Darnell, R. B. (2000) Nova-1 regulates neuron-specific alternative splicing and is essential for neuronal viability. *Neuron* **25**, 359-371.
25. Yano, M., Hayakawa-Yano, Y., Mele, A., and Darnell, R. B. (2010) Nova2 regulates neuronal migration through an RNA switch in disabled-1 signaling. *Neuron* **66**, 848-858.
26. Lai, M. C., Kuo, H. W., Chang, W. C., and Tarn, W. Y. (2003) A novel splicing regulator shares a nuclear import pathway with SR proteins. *EMBO J* **22**, 1359-1369.
27. McNeil, G. P., Zhang, X., Genova, G., and Jackson, F. R. (1998) A molecular rhythm mediating circadian clock output in *Drosophila*. *Neuron*. **20**, 297-303.
28. Lin, J. C., and Tarn, W. Y. (2005) Exon selection in alpha-tropomyosin mRNA is regulated by the antagonistic action of RBM4 and PTB. *Mol Cell Biol* **25**, 10111-10121.
29. Kar, A., Havlioglu, N., Tarn, W. Y., and Wu, J. Y. (2006) RBM4 interacts with



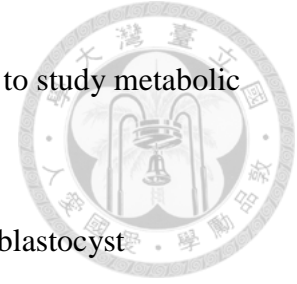
- an intronic element and stimulates tau exon 10 inclusion. *J Biol Chem* **281**, 24479-24488.
30. **Markus, M. A., and Morris, B. J.** (2009) RBM4: A multifunctional RNA-binding protein. *Int J Biochem Cell Biol* **41**, 740-743.
31. **Lin, J. C., and Tarn, W. Y.** (2011) RBM4 down-regulates PTB and antagonizes its activity in muscle cell-specific alternative splicing. *J Cell Biol* **193**, 509-520.
32. **Lin, J. C., Yan, Y. T., Hsieh, W. K., Peng, P. J., Su, C. H., and Tarn, W. Y.** (2013) RBM4 promotes pancreas cell differentiation and insulin expression. *Mol Cell Biol* **33**, 319-327.
33. **Lin, J. C., Lu, Y. H., Liu, Y. R., and Lin, Y. J.** (2016) RBM4a-regulated splicing cascade modulates the differentiation and metabolic activities of brown adipocytes. *Sci Rep* doi:10.1038/srep20665.
34. **Tarn, W. Y., Kuo, H. C., Yu, H. I., Liu, S. W., Tseng, C. T., Dhananjaya, D., Hung, K. Y., Tu, C. C., Chang, S. H., Huang, G. J., and Chiu, I. M.** (2016) RBM4 promotes neuronal differentiation and neurite outgrowth via Numb isoform expression. *Mol Biol Cell* **27**, 1676-1683.
35. **Wang, Y., Chen, D., Qian, H., Tsai, Y. S., Shao, S., Liu, Q., Dominguez, D., and Wang, Z.** (2014) The splicing factor RBM4 controls apoptosis, proliferation, and migration to suppress tumor progression. *Cancer Cell* **26**, 374-389.
36. **Jurica, M. S., Mesecar, A., Heath, P. J., Shi, W., Nowak, T., and Stoddard, B. L.** (1998) The allosteric regulation of pyruvate kinase by fructose-1,6-bisphosphate. *Structure* **6**, 195-210.
37. **Noguchi, T., Yamada, K., Inoue, H., Matsuda, T., and Tanaka, T.** (1987) The



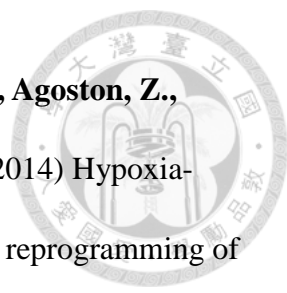
- L- and R- type isoenzymes of rat pyruvate kinase are produced from a single gene by use of different promoters. *J Biol Chem* **143**, 431-438.
38. **Noguchi, T., Inoue, H., and Tanaka, T.** (1986) The M1 and M2- type isoenzymes of rat pyruvate kinase are produced from the same gene by alternative RNA splicing. *J Biol Chem* **261**, 13807-13812.
39. **El-Maghrabi, M. R., Claus, T. H., McGrane, M. M., and Pilkis, S. J.** (1982) Influence of phosphorylation on the interaction of effectors with rat liver pyruvate kinase. *J Biol Chem* **257**, 233-237.
40. **Ashizawa, K., Willingham, M. C., Liang, C. M., and Cheng, S. Y.** (1991) In vivo regulation of monomer-tetramer conversion of pyruvate kinase subtype M2 by glucose is mediated via fructose 1,6-bisphosphate. *J Biol Chem* **266**, 16842-16846.
41. **Christofk, H. R., Vander Heiden, M. G., Wu, N., Asara, J. M., and Cantley, L. C.** (2008) Pyruvate kinase M2 is a phosphotyrosine-binding protein. **452**, 181-186.
42. **Christofk, H. R., Vander Heiden, M. G., Harris, M. H., Ramanathan, A., Gerszten, R. E., Wei, R., Fleming, M. D., Schreiber, S. L., and Cantley, L. C.** (2008) The M2 splice isoform of pyruvate kinase is important for cancer metabolism and tumour growth. *Nature* **452**, 230-233.
43. **Taniguchi, K., Ito, Y., Sugito, N., Kumazaki, M., Shinohara, H., Yamada, N., Nakagawa, Y., Sugiyama, T., Futamura, M., Otsuki, Y., Yoshida, K., Uchiyama, K., and Akao, Y.** (2015) Organ-specific PTB1-associated microRNAs determine expression of pyruvate kinase isoforms. *Sci Rep* doi:10.1038/srep08647.



44. **Clower, C. V., Chatterjee, D., Wang, Z., Cantley, L. C., Vander Heiden, M. G., Krainer, A. R.** (2010) The alternative splicing repressors hnRNP A1/A2 and PTB influence pyruvate kinase isoform expression and cell metabolism. *Proc Natl Acad Sci USA* **107**, 1894-1899.
45. **Alves-Filho, J. C., and Páissou-McDermott, E. M.** (2016) Pyruvate Kinase M2: A Potential Target for Regulating Inflammation. *Front Immunol*
doi:10.3389/immu.2016.00145.
46. **David, C. J., Chen, M., Assanah, M., Canoll, P., Manley, J. L.** (2010) HnRNP proteins controlled by c-Myc deregulate pyruvate kinase mRNA splicing in cancer. *Nature* **463**, 364-368.
47. **Rossi, D. J., Jamieson, C. H. M., and Weissman, I. L.** (2008) Stem cells and the pathways to aging and cancer. *Cell* **132**, 681-696.
48. **Folmes, C. D. L., Dzeja, P. P., Nelson, T. J., and Terzic, A.** (2012) Metabolic Plasticity in Stem Cell Homeostasis and Differentiation. *Cell Stem Cell* **11**, 596-606.
49. **Shyh-Chang, N., Daley, G. Q., and Cantley, L. C.** (2013) Stem cell metabolism in tissue development and aging. *Development* **140**, 2535-2547.
50. **Hanna, J. H., Saha, K., and Jaenisch, R.** (2010) Pluripotency and cellular reprogramming: Facts, hypotheses, unresolved issues. *Cell* **143**, 508-525.
51. **Zhang, J., Nuebel, E., Daley G. Q., Koehler, C. M., and Teitell, M. A.** (2012) Metabolic regulation in pluripotent stem cells during reprogramming and self-renewal. *Cell Stem Cell* **11**, 589-595.
52. **Barbehenn, E. K., Wales, R.G., and Lowry, O. H.** (1978) Measurement of

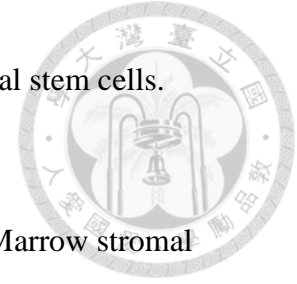


- metabolites in single preimplantation embryos; a new means to study metabolic control in early embryos. *J Embryo Exp Morphol* **43**, 29-46.
53. **Brinster, R. L., and Troike, D. E.** (1979) Requirements for blastocyst development in vitro. *J Anim Sci* **49**, 26-34.
54. **Johnson, M. T., Mahmood, S., Patel, M. S.** (2003) Intermediary metabolism and energetics during murine early embryogenesis. *J Biol Chem* **278**, 31457-31460.
55. **Facucho-Oliveira, J. M., Alderson, J., Spikings, E. C., Egginton, S., and St John, J. C.** (2007) Mitochondrial DNA replication during differentiation of murine embryonic stem cells. *J Cell Sci* **120**, 4025-4034.
56. **Chen, C. T., Shih, Y. R., Kuo, T. K., Lee, O. K., and Wei, Y. H.** (2008) Coordinated changes of mitochondrial biogenesis and antioxidant enzymes during osteogenic differentiation of human mesenchymal stem cells. *Stem Cells* **26**, 960-968.
57. **Takubo, K., Nagamatsu, G., Kobayashi, C. I., Nakamura-Ishizu, A., Kobayashi, H., Ikeda, E., Goda, N., Rahimi, Y., Johnson, R. S., Soga, T., Hirao, A., Suematsu, M., and Suda, T.** (2013) Regulation of glycolysis by Pdk functions as a metabolic checkpoint for cell cycle quiescence in hematopoietic stem cells. *Cell Stem Cell* **12**, 49-61.
58. **Folmes, C. D., Nelson, T. J., Martinez-Fernandez, A., Arrell, D. K., Lindor, J. Z., Dzeja, P. P., Ikeda, Y., Perez-Terzic, C., and Terzic, A.** (2011) Somatic oxidative bioenergetics transitions into pluripotency-dependent glycolysis to facilitate nuclear reprogramming. *Cell Metab* **14**, 264-271.

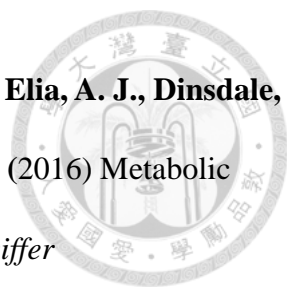
- 
59. **Mathieu, J., Zhou, W., Xing, Y., Sperber, H., Ferreccio, A., Agoston, Z., Kuppusamy, K. T., Moon, R. T., and Ruohola-Baker, H.** (2014) Hypoxia-inducible factors have distinct and stage-specific roles during reprogramming of human cells to pluripotency. *Cell Stem Cell* **14**, 592-605.
60. **Hanover, J. A., Krause, M. W., and Love, D. C.** (2012) Bittersweet memories: linking metabolism to epigenetics through O-GlcNAcylation. *Nat Rev Mol Cell Biol* **13**, 312-321.
61. **Jang, H., Kim, T. W., Yoon, S., Choi, S. Y., Kang, T. W., Kim, S. Y., Kwon, Y. W., Cho, E. J., and Youn, H. D.** (2012) O-GlcNAc regulates pluripotency and reprogramming by directly acting on core components of the pluripotency network. *Cell Stem Cell* **11**, 62-74.
62. **Shyh-Chang, N., Locasale, J. W., Lyssiotis, C. A., Zheng, Y., Teo, R. Y., Ratanasirinrawoot, S., Zhang, J., Onder, T., Unternaehrer, J. J., Zhu, H., Asara, J. M., Daley, G. Q., and Cantley, L. C.** (2013) Influence of threonine metabolism on S-adenosylmethionine and histone methylation. *Science* **339**, 222-226.
63. **Homem, C. C.F., Steinmann, V., Burkard, T.R., Jais, A., Esterbauer, H., and Knoblich, A.** (2014) Ecdysone and Mediator change energy metabolism to terminate proliferation in Drosophila neural stem cells. *Cell* **158**, 874-888.
64. **Lange, C., Garcia, M. T., Decimo, I., Bifari, F., Eelen, G., Quaegebeur, A., Boon, R., Zhao, H., Boeckx, B., Chang, J., Wu, C., Le Nobel, F., Lambrechts, D., Dewerhin, M., Kuo, C. J., Huttner, W. B., and Carmeliet, P.** (2016) Relief of

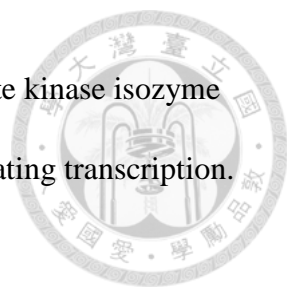


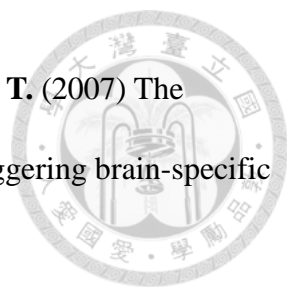
- hypoxia by angiogenesis promotes neural stem cell differentiation by targeting glycolysis. *EMBO J* **35**, 924-941.
65. **Bartesaghi, S., Graziano, V., Galavotti, S., Henriquez, N. V., Betts, J., Saxena, J., Deli, A., Karlsson, A., Martins, L. M., Capasso, M., Nicotera, P., Brandner, S., De Laurenzi, V., and Salomoni, P.** (2015) Inhibition of oxidative metabolism leads to p53 genetic inactivation and transformation in neural stem cells. *PNAS* **112**, 1059-1064.
66. **Kim, H., Jang, H., Kim, T. W., Kang, B. H., Lee, S. E., Jeon, Y. K., Chung, D. H., Choi, J., Shin, J., Cho, E. J., and Youn, H. D.** (2015) Core pluripotency factors directly regulate metabolism in embryonic stem cell to maintain pluripotency. *Stem Cells* **33**, 2699-2711.
67. **Bélanger, M., Allaman, I., and Magistretti, P.J.** (2011) Brain energy metabolism: focus on astrocyte-neuron metabolic cooperation. *Cell Metab* **14**, 724-738.
68. **Friedenstein, A. J., Chailakhyan, R.K., Latsinik, N. V., Panasyuk, A. F., and Keiliss-Borok, I. V.** (1974) Stromal cells responsible for transferring the microenvironment of the hemopoietic tissues. Cloning *in vitro* and retransplantation *in vivo*. *Transplantation* **17**, 331-340.
69. **Caplan, A. I.** (1991) Mesenchymal stem cells. *J Orthop Res* **9**, 641-650.
70. **Uccelli, A., Moretta, L., and Pistoia, V.** (2008) Mesenchymal stem cells in health and disease. *Nat Rev Immunol* **8**, 726-736.
71. **Pittenger, M. F., Mackay, A. M., Beck, S. C., Jaiswai, R. K., Douglas, R., Mosca, J. D., Moorman, M. A., Simonetti, D. W., Craig, S., and Marshak, D,**



- R.** (1999) Multilineage potential of adult human mesenchymal stem cells. *Science* **284**, 143-147.
72. **Kopen, G. G., Prockop, D. J., and Phinney, D. G.** (1999) Marrow stromal cells migrate throughout forebrain and cerebellum, and they differentiate into astrocytes after injection into neonatal mouse brains. *Proc Natl Acad Sci USA* **96**, 10711-10716.
73. **Joyce, N., Annett, G., Wirthlin, L., Olson, S., Bauer, G., and Nolte, J. A.** (2010) Mesenchymal stem cells for the treatment of neurodegenerative disease. *Regen Med* **5**, 933-946.
74. **Wellen, K. E., Hatzivassiliou, G., Sachdeva, U.M., Bui, T.V., Cross, J. R., Thompson, C. B.** (2009) ATP-citrate lyase links cellular metabolism to histone acetylation. *Science* **324**, 1076-1080.
75. **Pattappa, G., Heywood, H. K., deBruijn, J. D., Lee, D. A.** (2011) The metabolism of human mesenchymal stem cells during proliferation and differentiation. *J Cell Physiol* **226**, 2562-2570.
76. **Chen, M., David, C. J., and Manley, J.L.** (2012) Concentration-dependent control of pyruvate kinase M mutually exclusive splicing by hnRNP proteins. *Nat Struct Mol Biol* **19**, 346-354.
77. **Tsai, C. C., Chen, C. L., Liu, H. C., Lee, Y. T., Wang, H. W., Hou, L. T., and Hung, S.C.** (2010) Overexpression of hTERT increases stem-like properties and decreases spontaneous differentiation in human mesenchymal stem cell lines. *J Biomed Sci* doi:10.1186/1423-0127-17-64.

- 
78. **Agostini, M., Romeo, F., Inoue, S., Niklisin-Chirou, M. V., Elia, A. J., Dinsdale, D., Morone, N., Knight, R. A., Mak, T. W., and Melino, G.** (2016) Metabolic reprogramming during neuronal differentiation. *Cell Death Differ*
doi:10.1038/cdd.2016.36.
79. **Nakashima, K., Takizawa, T., Ochiai, W., Yanagisawa, M., Hisatsune, T., Nakafuku, M., Miyazono, K., Kishimoto, T., Kageyama, R., and Taga, T.** (2001) BMP2-mediated alteration in the developmental pathway of fetal mouse brain cells from neurogenesis to astrocytogenesis. *Proc Natl Acad Sci U S A* **8**, 5868-5873.
80. **Wang, Y., Yang, J., Li, H., Wang, X., Zhu, L., Fan, M., and Wang, X.** (2013) Hypoxia promotes dopaminergic differentiation of mesenchymal stem cells and shows benefits for transplantation in a rat model of Parkinson's disease. *PLoS One*
doi:1371/journal.pone.0054296.
81. **Jeon, E. S., Shin, J. H., Hwang, S. J., Moon, G. J., Bang, O. Y., and Kim, H. H.** (2014) Cobalt chloride induces neuronal differentiation of human mesenchymal stem cells through upregulation of microRNA-124a. *Biochem Biophys Res Commun* **444**, 581-587.
82. **Luo, W., Hu, H., Chang, R., Zhong, J., Knable, M., O'Meally, R., Cole, R. N., Pandey, A., and Semenza, G. L.** (2011) Pyruvate kinase M2 is a PHD3-stimulated coactivator for hypoxia-inducible factor 1. *Cell* **145**, 732-744.
83. **Gueroussov, S., Gonatopoulos-Pournatzis, T., Irimia, M., Raj, B., Lin, Z. Y., Gingras, A. C., and Blencowe, B.J.** (2015) An alternative splicing event amplifies evolutionary differences between vertebrates. *Science* **349**, 868-873.

- 
84. **Lee, J., Kim, H. K., Han, Y.M., and Kim, J.** (2008) Pyruvate kinase isozyme type M2 (PKM2) interacts and cooperates with Oct4 in regulating transcription. *Int J Biochem Cell Biol* **40**, 1043-1054.
85. **Yang, W., Xia, Y., Hawke, D., Li, X., Liang, J., Xing, D., Aldape, K., Hunter, T., Alfred Yung, W. K., and Lu, Z.** (2012) PKM2 phosphorylates histone H3 and promotes gene transcription and tumorigenesis. *Cell* **150**, 685-696.
86. **Zhang, Y., Chen, K., Sloan, S. A., Bennett, M. L., Scholze, A. R., O’Keeffe, S., Phatnani, H. P., Guarnieri, P., Caneda, C., Ruderisch, N., Deng, S., Liddelow, S. A., Zhang, C., Daneman, R., Maniatis, T., Barres, B. A., and Wu, J. Q.** (2014) An RNA-sequencing transcriptome and splicing database of glia, neurons, and vascular cells of the cerebral cortex. *J Neurosci* **34**, 11929-11947.
87. **Mohyeldin, A., Garzón-Muvdi, T., and Quiñones-Hinojosa, A.** (2010) Oxygen in stem cell biology: a critical component of the stem cell niche. *Cell Stem Cell* **7**, 150-161.
88. **Vieira, H. L., Alves, P. M., and Vercelli, A.** (2011) Modulation of neuronal stem cell differentiation by hypoxia and reactive oxygen species. *Prog Neurobiol* **93**, 444-455.
89. **Pacary, E., Legros, H., Valable, S., Duchatelle, P., Lecocq, M., Petit, E., Nicole, O., and Bernaudin, M.** (2006) Synergistic effect of CoCl₂ and ROCK inhibition on mesenchymal stem cell differentiation into neuron-like cells. *J Cell Sci* **199**, 2667-2678.

- 
90. **Makeyev, E. V., Zhang, J., Carrasco, M. A., and Maniatis, T.** (2007) The microRNA miR-124 promotes neuronal differentiation by triggering brain-specific alternative pre-mRNA splicing. *Mol Cell* **27**, 435-448.
91. **Lou, C. H., Shao, A., Shum, E. Y., Espinoza, J. L., Huang, L., Katam, R., and Wilkinson, M. F.** (2014) Posttranscriptional control of the stem cell and neurogenic programs by the nonsense-mediated RNA decay pathway. *Cell Rep* **6**, 748-764.

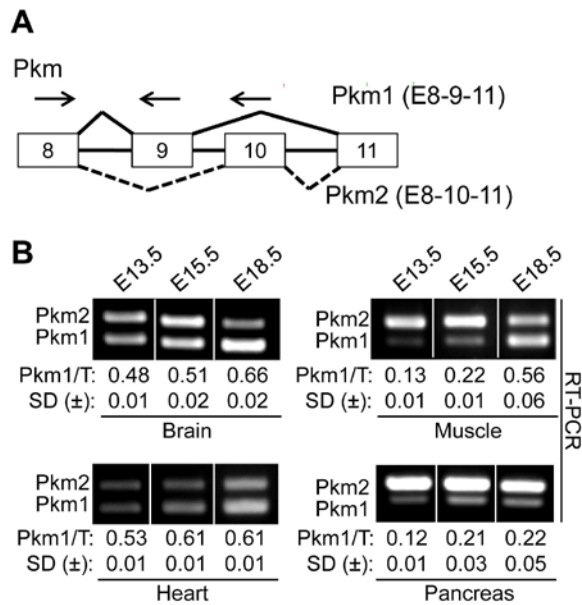


Figure 1. Pkm isoform switched during mouse embryo development. (A) Schematic diagram of alternative splicing of the mouse Pkm gene. Arrows depict primers used in RT-PCR (Table 1). (B) Total RNA was extracted from indicated mouse tissues at indicated embryonic days and subjected to RT-PCR analysis using primers as depicted in panel A. Representative lanes were spliced from original gels (Fig. 2B, C). The relative levels of Pkm1 vs. total Pkm transcripts (T) are shown below the gels; the average values and standard deviation were obtained from 2-3 sets of samples.

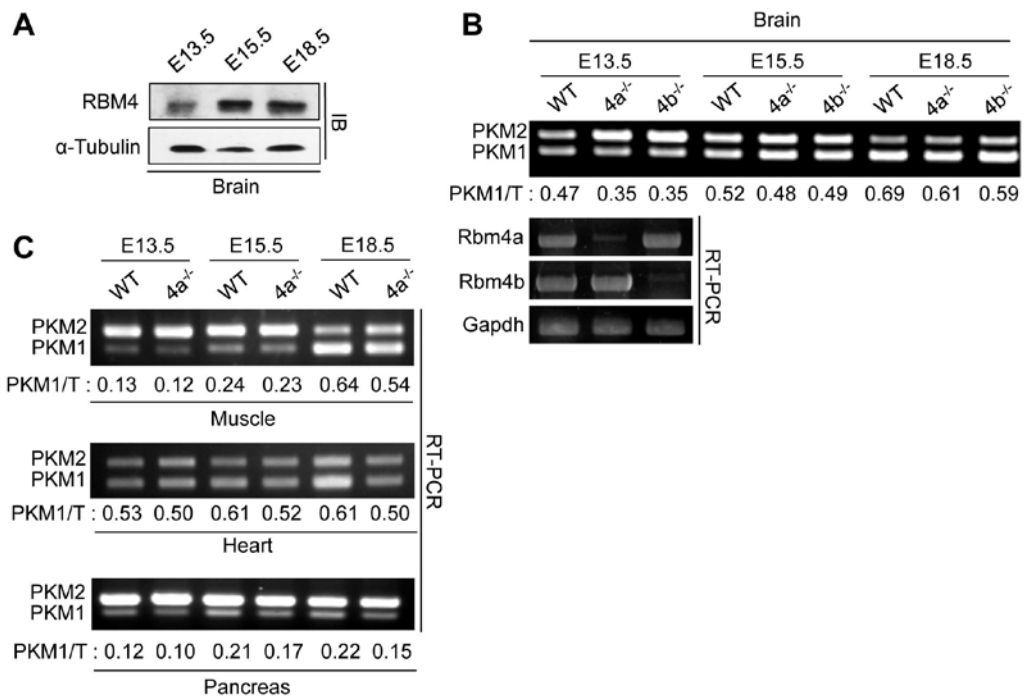


Figure 2. RBM4 significantly affects Pkm isoform switch in highly energy-consuming tissues. (A) The RBM4 expression was analyzed by immunoblotting from the embryonic brain lysates at indicated embryonic days. α -Tubulin was used as control. (B) RT-PCR was performed in wild type, *Rbm4a* or *Rbm4b* knockout embryonic brains at indicated embryonic days to detect the expression of Pkm isoforms. *Rbm4a*, *Rbm4b*, and *Gapdh* (as a control) were detected at E13.5 day. (C) RT-PCR of Pkm in wild type or *Rbm4a* knockout embryonic tissues (muscle, heart, and pancreas). The average PKM1 vs. total PKM ratios shown below the gels were obtained from 2-3 sets of samples.

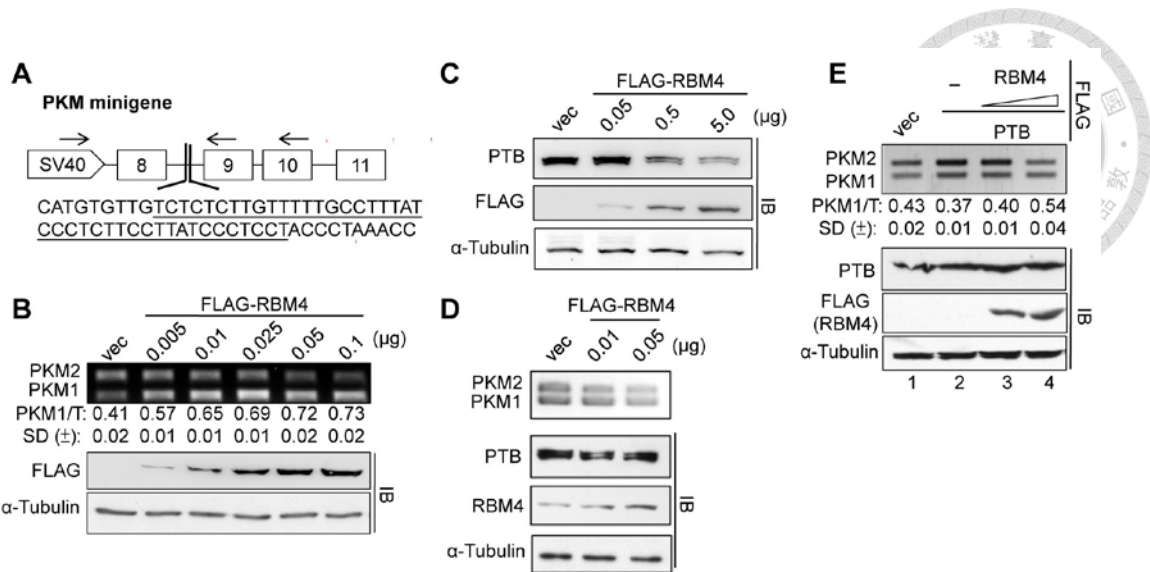


Figure 3. RBM4 regulates alternative splicing of PKM not by suppressing PTB protein expression. (A) Schematic diagram of the PKM minigene spanning exons 8 to 11 of mouse Pkm. A CU-rich region (61 nt) in intron 8 was used as probe for EMSA; the underlined region (42 nt) was deleted in the mutant reporter. Arrows depict primers used in RT-PCR (Table 1). (B) HEK293T cells were transfected with indicated amounts of the FLAG-RBM4 expression vector or the empty vector (0.1 µg). (C) HEK293T cells were transfected with indicated amounts of the FLAG-RBM4 expression vector or the empty vector (5.0 µg). (D) HEK293T cells were transfected with indicated amounts of the FLAG-RBM4 expression vector or the empty vector (0.05 µg). (E) The PKM minigene was co-transfected with empty vector (lane 1) or 1 µg of the FLAG-PTB vector and 0, 1 or 2 µg of the FLAG-RBM4 vector (lanes 2-4) into HEK293T cells. For panels B and E, the relative levels of PKM1 vs. total PKM were calculated as in Fig. 1. The average values and standard deviation were obtained from three independent experiments. Immunoblotting (IB) was performed using antibodies against PTB, α-Tubulin, RBM4, and FLAG tag.

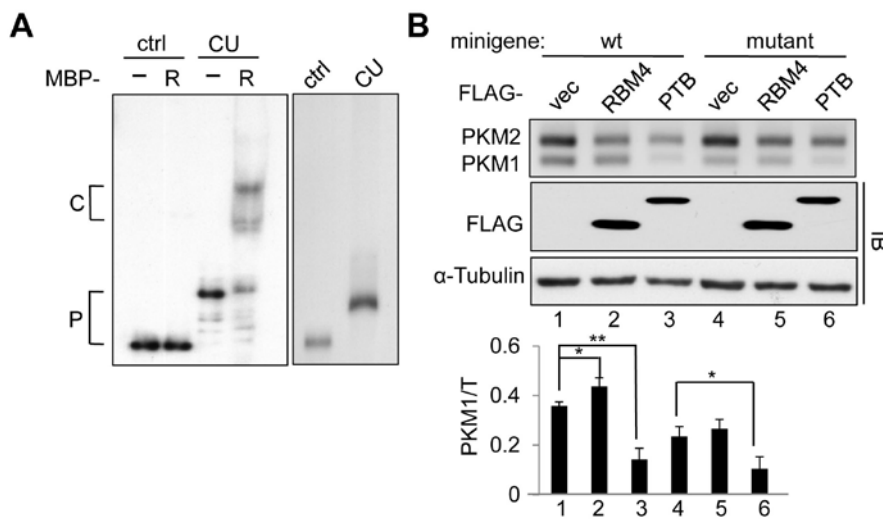


Figure 4. RBM4 regulates alternative splicing of PKM pre-mRNA via an intronic CU-rich sequence. (A) For EMSA, ^{32}P -labeled control or CU-rich probe was incubated with recombinant MBP (-) or MBP-RBM4 (R) protein, and then analyzed by non-denaturing polyacrylamide gel electrophoresis (C: RNA-protein complex; P: free probe). (B) HEK293T cells were co-transfected with an expression vector (empty, 0.1 μg of FLAG-RBM4 or 0.5 μg of FLAG-PTB) and the PKM minigene (wild type or mutant). Bar graph shows the relative level of PKM1 over total PKM; the average and standard deviation were obtained from three experiments (p -value: * < 0.05, ** < 0.01).

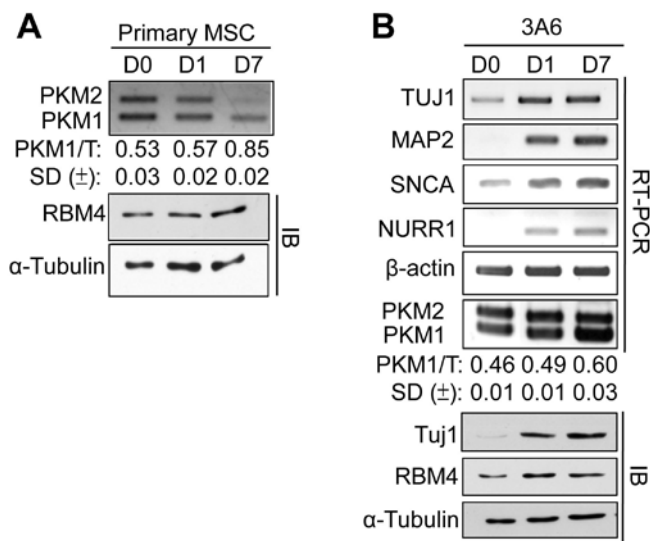


Figure 5. RBM4 expression and the alternative splicing of PKM pre-mRNA is correlates to the neuronal differentiation of MSCs. (A) Primary human mesenchymal stem cells (MSCs) or (B) 3A6 cells were cultured in the neuronal differentiation medium up to 7 days (D0 to D7). The expression neuronal genes as indicated were detected by RT-PCR using specific sets of primers (Table 1). Immunoblotting (IB) was performed using antibodies against Tuj1, RBM4 and α-Tubulin. For panel A and B, the PKM isoforms were detected and relative ratios were calculated as in Fig. 1A except that human PKM primers were used.

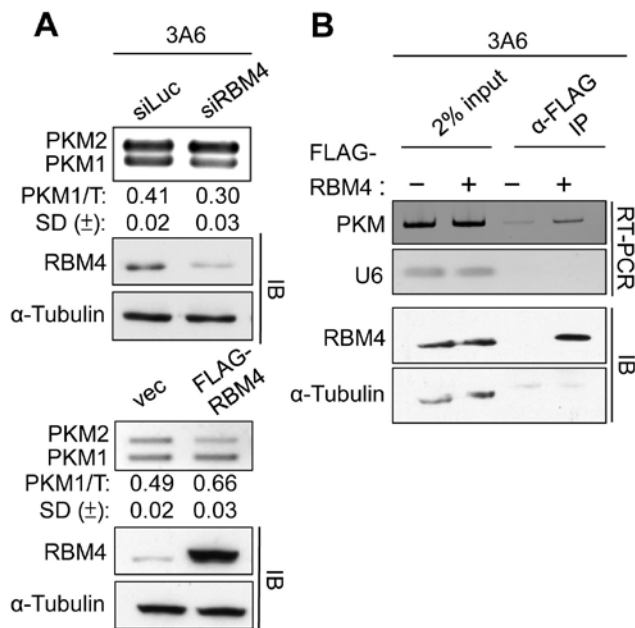


Figure 6. RBM4 regulates the PKM splice isoform switch of MSCs. (A) 3A6 cells were transfected with siRBM4 (siLuc as control) or the FLAG-RBM4 or empty expression vector for 2 days and 30 hrs, respectively. The PKM isoforms were detected and relative ratios were calculated as in Fig. 5. (B) Mock or FLAG-RBM4-expressing 3A6 cell lysates were subjected to immunoprecipitation using anti-FLAG. RT-PCR was performed to detect co-precipitated PKM transcripts; U6 snRNA was used as control. For panel A and B, immunoblotting (IB) was performed using antibodies against RBM4 and α -Tubulin.

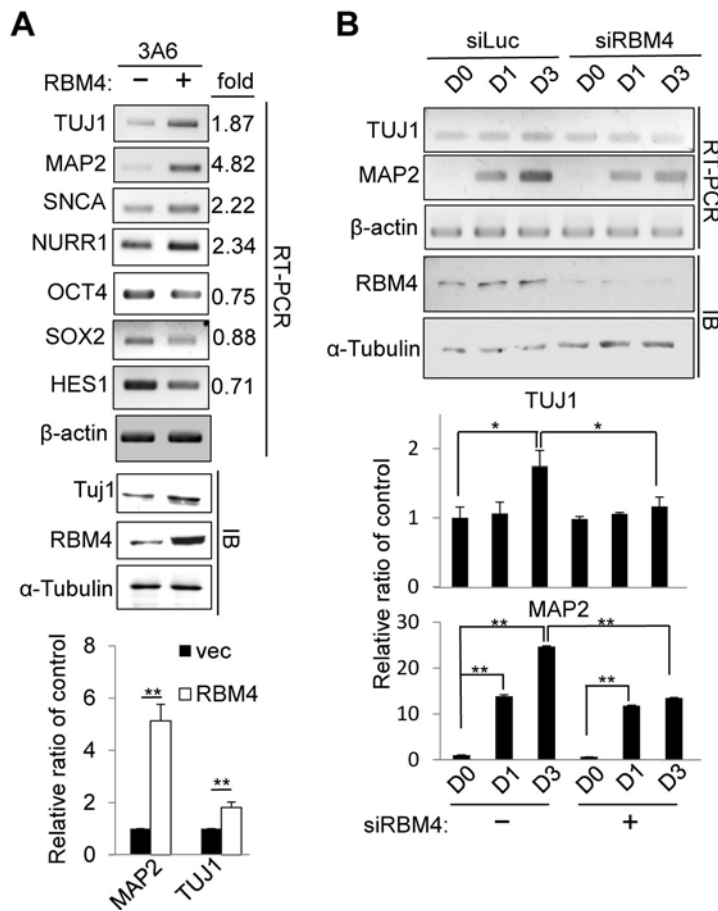


Figure 7. RBM4 promotes neuronal differentiation of MSCs. (A) 3A6 cells were transfected with the empty or FLAG-RBM4 expression vector. Thirty hours after transfection, the expression of indicated genes was detected by RT-PCR (Table 1). Immunoblotting (IB) was performed using antibodies against Tuj1, RBM4 and α -Tubulin. Fold changes are at the right side. Bar graph shows RT-qPCR of MAP2 and TUJ1. (B) 3A6 cells were transfected with siRBM4 or siLuc. Cells were collected 24 hrs post-transfection (D0) or after incubation in NIM up to 3 days (D1 and D3). TUJ1, MAP2 and β -actin (as control) mRNAs were detected by using RT-PCR (Table 1). Immunoblotting (IB) was performed using antibodies against RBM4 and α -Tubulin. Bar graph shows the relative level of each gene as compared to the control. For all bar graphs, the average value and standard deviation were obtained from three independent experiments (p -value: * < 0.05; ** < 0.01).

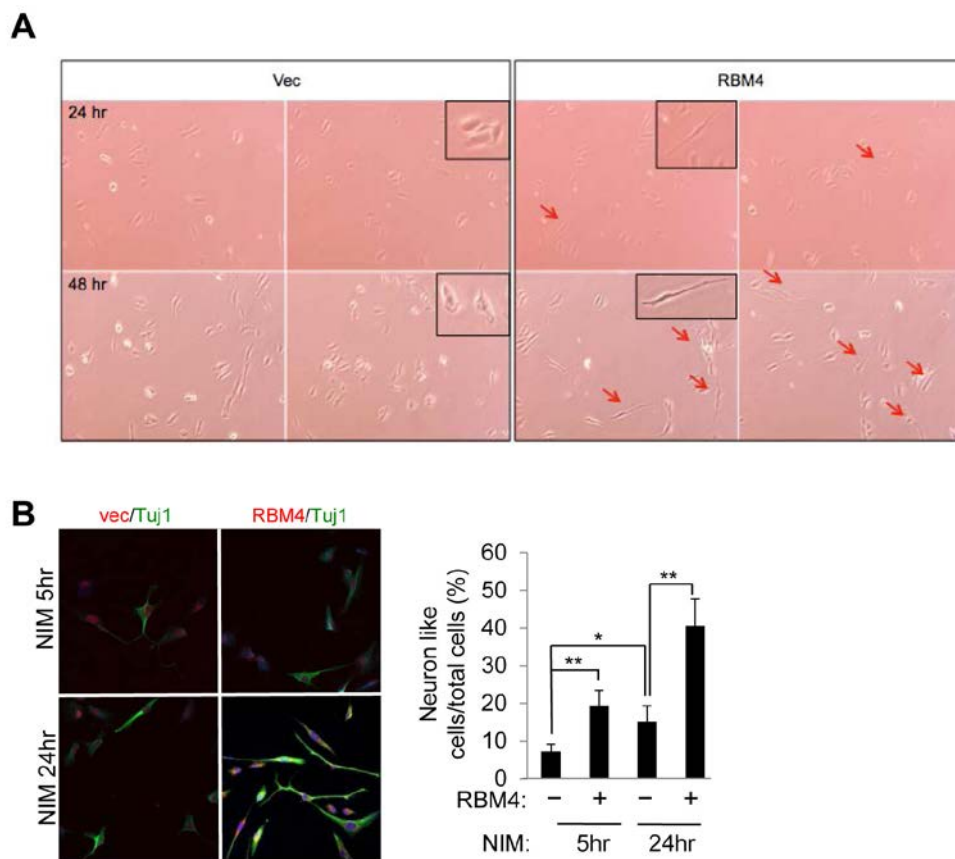


Figure 8. RBM4 enhances neurite outgrowth of MSCs. (A) 3A6 cells were transfected with the FLAG-RBM4 expression vector (empty vector as control) for 24 or 48 hours. Arrows depict the neurites of 3A6 cells. (B) 3A6 cells were transfected with the empty or FLAG-RBM4 expression vector for 30 hours and then cultured in NIM for 5 or 24 hours. Indirect immunofluorescence was performed using antibodies against Tuj1 and FLAG tag. Cells with a Tuj1-positive neurite whose length was ≥ 2 -fold that of the cell body were defined as neuron-like cells. Bar graph shows the percentages of neuron-like cells in each group. The average value and standard deviation were obtained from three independent experiments (p -value: * < 0.05 ; ** < 0.01).

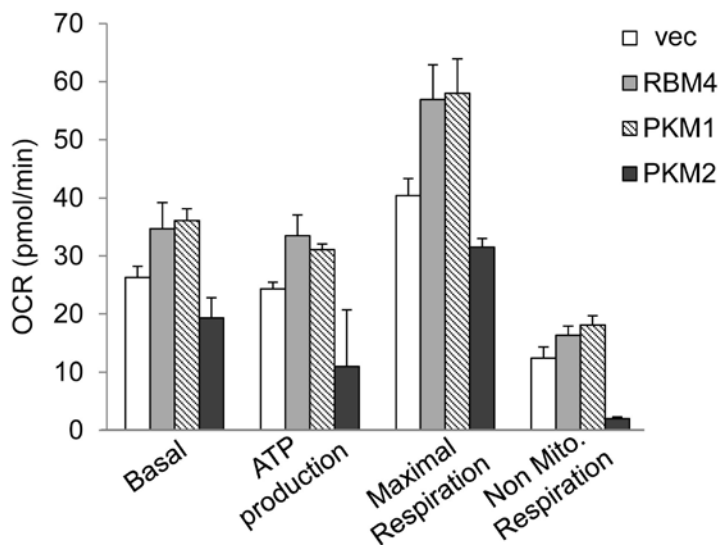


Figure 9. RBM4-regulated PKM1 isoform expression enhances mitochondrial OXPHOS of MSCs. 3A6 cells were transfected with the expression vector (empty, FLAG-RBM4, -PKM1 or -PKM2) for 30 hours. The oxygen consumption rate was detected by the Seahorse XF metabolism analysis system. Bar graph shows the OCR (pmol/min) at different cellular metabolic status in each group. The average and standard deviation were obtained from three independent experiments.

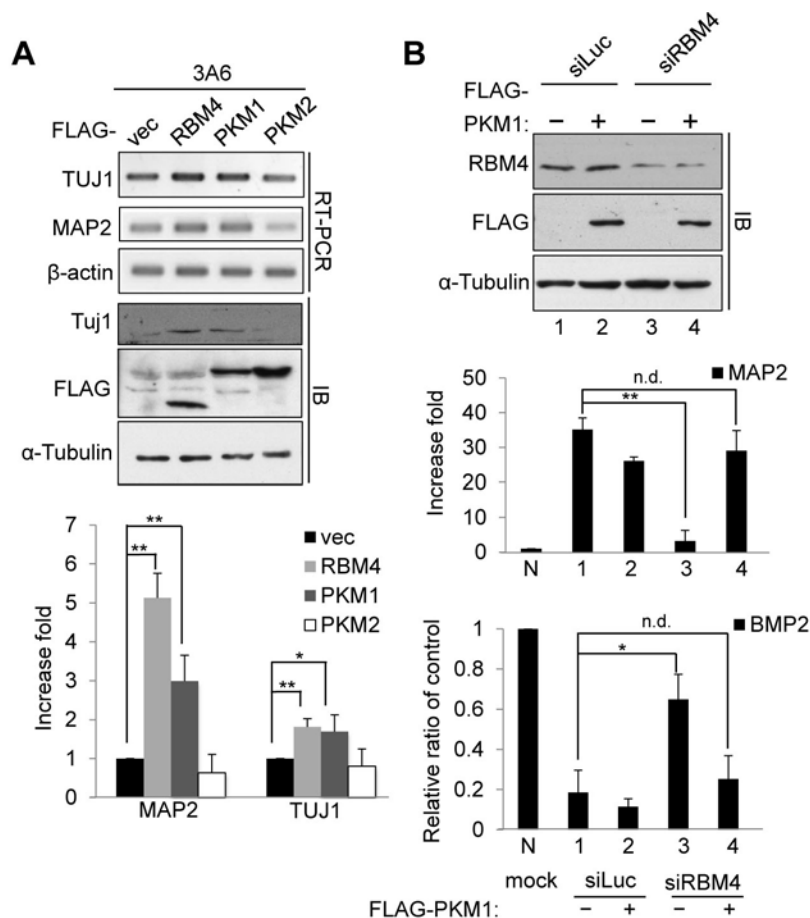


Figure 10. The switch of PKM isoforms contributes to neuronal differentiation of MSCs. (A) 3A6 cells were transfected as Fig. 9. RT-PCR was performed as in Fig. 7B. Immunoblotting (IB) was performed using antibodies against Tuj1, FLAG tag and α -Tubulin. Bar graph shows RT-qPCR of MAP2 and TUJ1 as in Fig 7B. (B) 3A6 cells were co-transfected with control or RBM4 siRNA with the empty or FLAG-PKM1 expression vector, followed by neuronal differentiation for 3 days. Bar graphs show the expression of MAP2 (top panel) and BMP2 (bottom panel). N represents mock transfected and undifferentiated cells. Average was obtained from 3 times of experiments. For all bar graphs, the average value and standard deviation were obtained from three independent experiments (p -value: * < 0.05; ** < 0.01; n.d.: no significant differences).

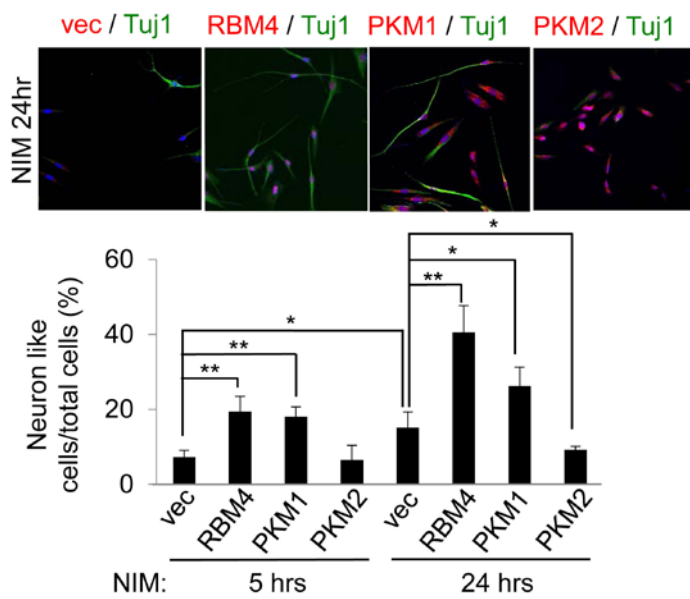


Figure 11. PKM1 enhances the neurite outgrowth of MSCs as RBM4. (B) 3A6 cells were transfected as Fig. 9, followed by culture in NIM for 5 or 24 hours. Indirect immunofluorescence staining was performed as in Fig. 8B; representative images of 24 hr are shown. Bar graph shows the percentage of neuron-like cells in each group. The average value and standard deviation were obtained from three independent experiments (p -value: * < 0.05; ** < 0.01).

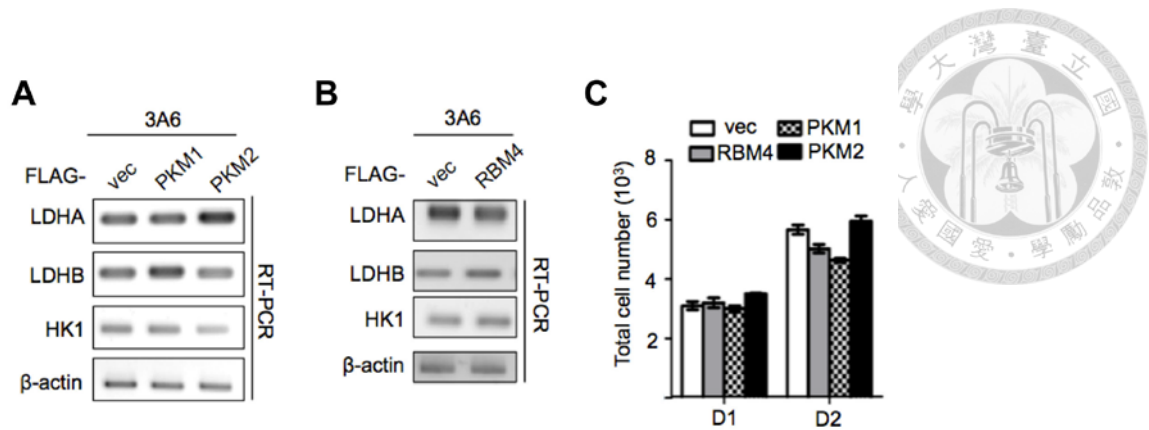


Figure 12. RBM4 and PKM1 change glycolytic-enzyme gene expression and cell growth rate. (A) 3A6 cells were transfected with the expression vector (empty, FLAG-PKM1, -PKM2) for 30 hours. (B) 3A6 cells were transfected with the expression vector (empty, FLAG-RBM4) as in panel A. In panel A and B, the expression of glycolytic-enzyme genes as indicated was detected by RT-PCR using specific sets of primers (Table 1). (C) 3A6 cells were transfected with the expression vector (empty, FLAG-RBM4, -PKM1 or -PKM2) for 30 hours. 1×10^3 of transfected cells were re-seeded in 98 well culture dish for 1 and 2 days. The cell growth was analysis by CCK-8 kit to count the total cell number.

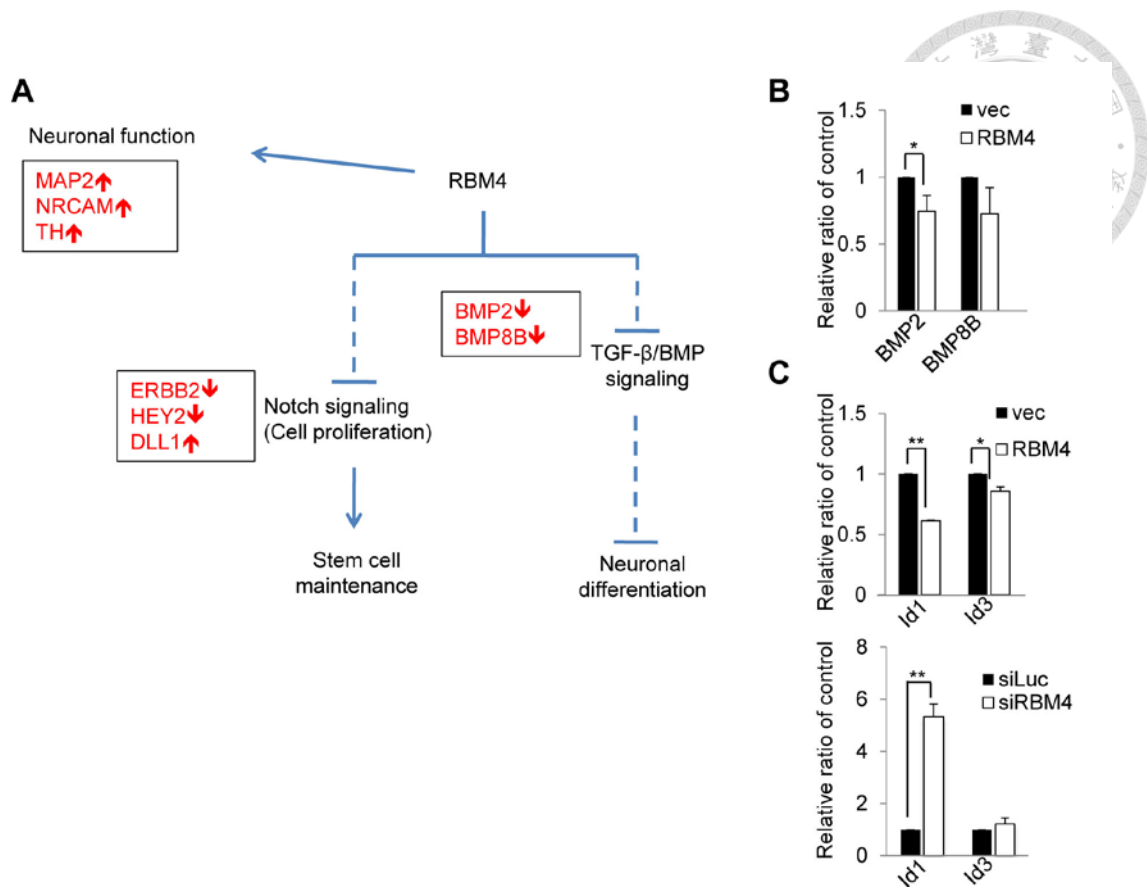


Figure 13. RBM4 promotes neuronal differentiation via suppressing a negative regulating pathway of MSCs. (A) 3A6 cells were transfected with the FLAG-RBM4 or empty vector for 30 hours followed by culture in NIM for 0 and 24 hours. 84 genes involving in neurogenesis were analysis by using qPCR array kit (PAHS-404Z, QIAGEN). Arrows in the box depict the up- or down- regulation of indicated genes, which modulated by RBM4. Blue lines indicate the potential signaling pathway regulated by RBM4. Dashed lines depict a repress effect. (B) 3A6 cells were transfected as in panel A. The expression of BMP2 and BMP8B (top panel) was detected by RT-qPCR. (C) 3A6 cells were transfected with the empty or FLAG-RBM4 expression vector (middle panel) or siRNA (siRBM4 or siLuc as control, bottom panel). The expression of Id1 and Id3 was detected by RT-qPCR. Bar graph shows the relative expression level of each gene as compared to the control. The average value and standard deviation were obtained from three independent experiments (p -value: * < 0.05; ** < 0.01).

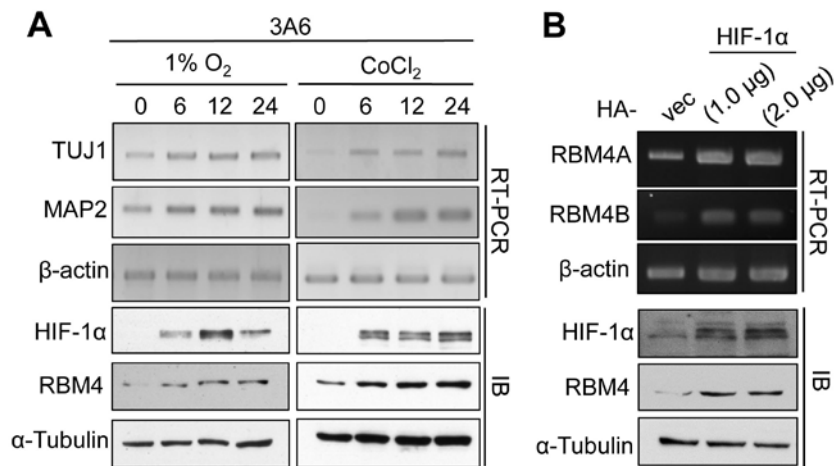


Figure 14. Hypoxia environment induces RBM4 expression and neuronal differentiation of MSCs. (A) 3A6 cells were incubated under hypoxic conditions (1% O₂) (left) or treated with 200 μM CoCl₂ (right) for 6, 12, and 24 hours (0 hr as control). RT-PCR was performed as in Fig. 7B. (B) 3A6 cells were transfected with empty or HA-tagged HIF-1a vector. RBM4A, RBM4B and β-actin mRNAs were detected using RT-PCR. For panel A and B, immunoblotting (IB) was performed using antibodies against HIF-1a, RBM4 and α-Tubulin.

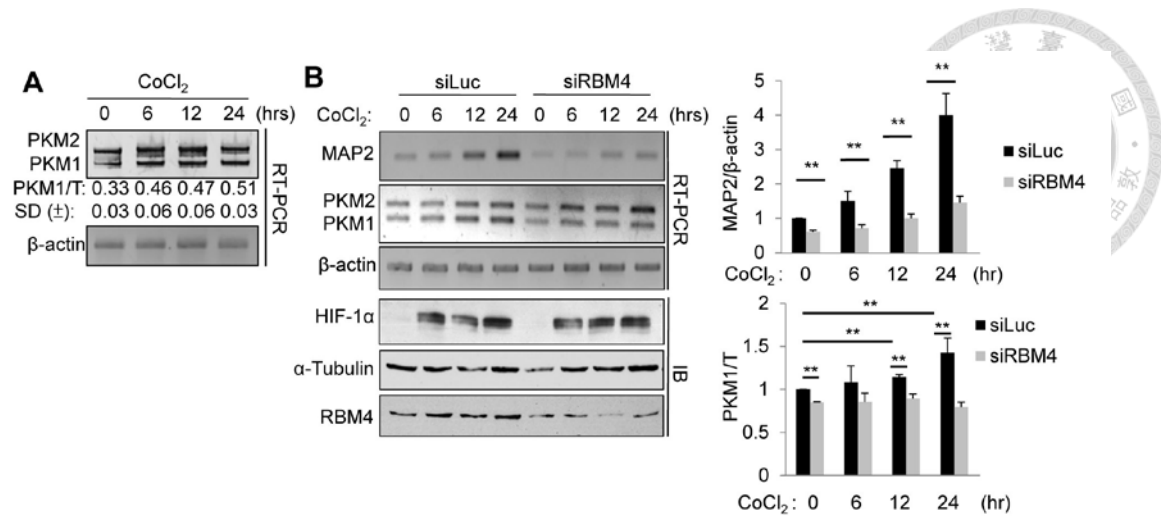


Figure 15. RBM4 is involved in the hypoxia-induced switch of PKM splice isoforms and neuronal differentiation. (A) 3A6 cells were treated with CoCl₂ as in Fig. 14A. PKM isoforms were detected and the PKM1/total PKM ratios are shown below the gels as in Fig. 1 (B) 3A6 cells were transfected with siLuc or siRBM4 for 2 days and then treated with CoCl₂ as in panel A. The expression of MAP2 and PKM isoforms was detected by RT-PCR. Immunoblotting (IB) was performed using antibodies against HIF-1α, RBM4 and α-Tubulin. Bar graphs show the relative MAP2 expression level (top) and PKM1/total PKM (T) ratio (bottom). The average value and standard deviation were obtained from three independent experiments (*p*-value: ** < 0.01).

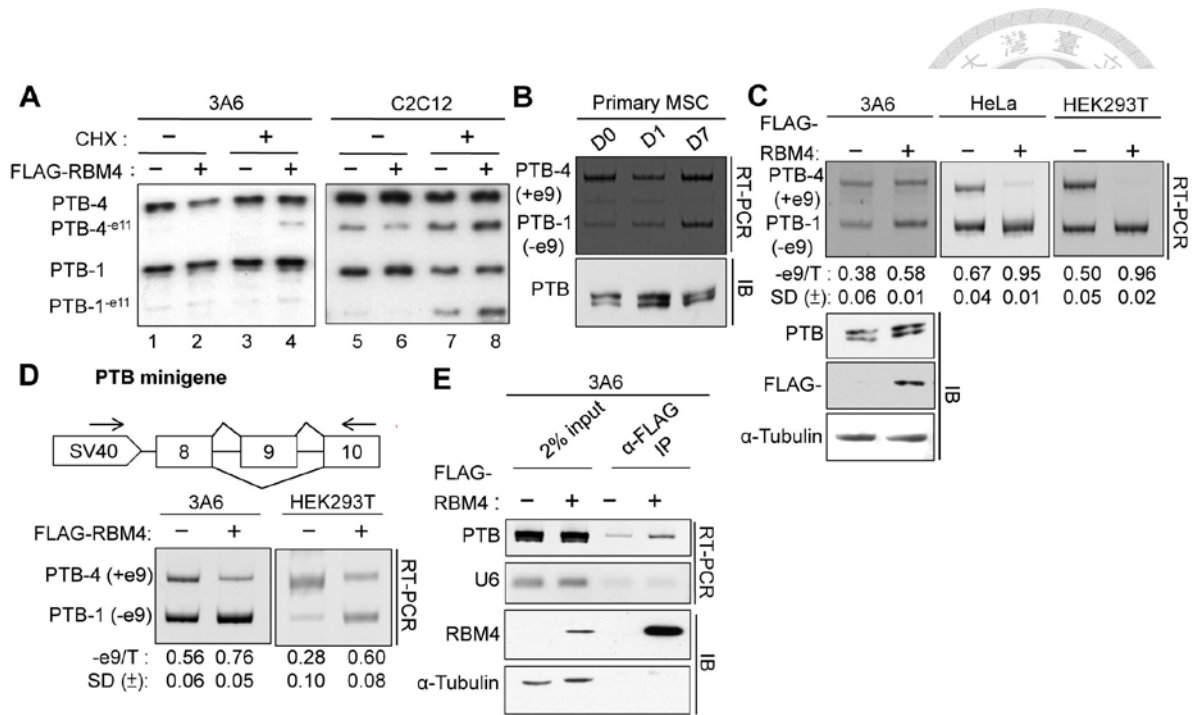


Figure 16. RBM4 modulates PTB isoform expression during neuronal differentiation of MSCs. (A) 3A6 cells or C2C12 myoblast were transfected with the empty or FLAG-RBM4 expression vector. Thirty hours post-transfection, cells were mock treated or treated with 100 μ M cycloheximide (CHX) for 2 hours before harvest. Total RNA was subjected to RT-PCR analysis using primers specific for exons 8 and 12 of human PTB (Table 1). (B) Primary human MSCs were cultured as in Fig. 5A. Total RNA was analyzed using primers as in panel A. Immunoblotting (IB) was performed using anti-PTB. (C) 3A6 cells, HeLa cells and HEK293T cells were transfected as in panel A. RT-PCR was as in panel A. Immunoblotting was performed using anti-PTB, anti-FLAG and α -Tubulin. (D) Schematic diagram of the PTB minigene spanning exons 8 to 10 of human PTB. 3A6 cells and HEK293T cells were co-transfected with the expression vector (empty or FLAG-RBM4) and PTB minigene. PTB isoform expression was detected by RT-PCR using specific primers as depicted. The relative levels of PTB-e9 (PTB-1) vs. total PTB are shown below the gels; average and standard deviation were obtained from three independent experiments. (E) Immunoprecipitation was performed as in Fig. 6B, followed by RT-PCR using PTB primers; U6 was as control.

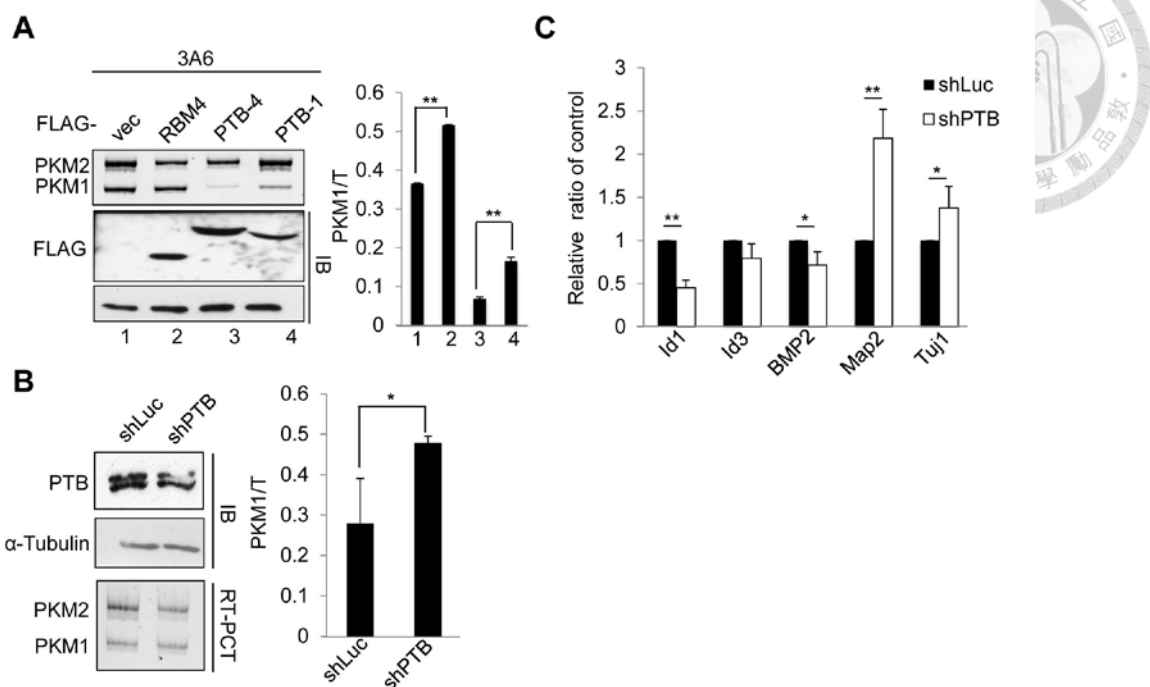


Figure 17. RBM4 induces the expression of a PTB isoform with attenuated splicing activity in human MSCs. (A) The PKM minigene was transfected with the empty vector or the vector expressing FLAG-RBM4 or -PTB-4 (+e9) or -PTB-1 (-e9). PT-PCR and immunoblotting were performed. Bar graph shows PKM1 vs. total PKM (n=3). (B) 3A6 cells were transfected with the shLuc (control) or shPTB expression vector. Left panel shows immunoblotting of PTB and α -Tubulin and RT-PCR of PKM. Bar graph shows the PKM1 to total PKM ratio. (C) RT-qPCR of indicated genes was performed in the above transfectants. Averages were obtained from three times of experiments; *p*-value: * < 0.05; ** < 0.01.

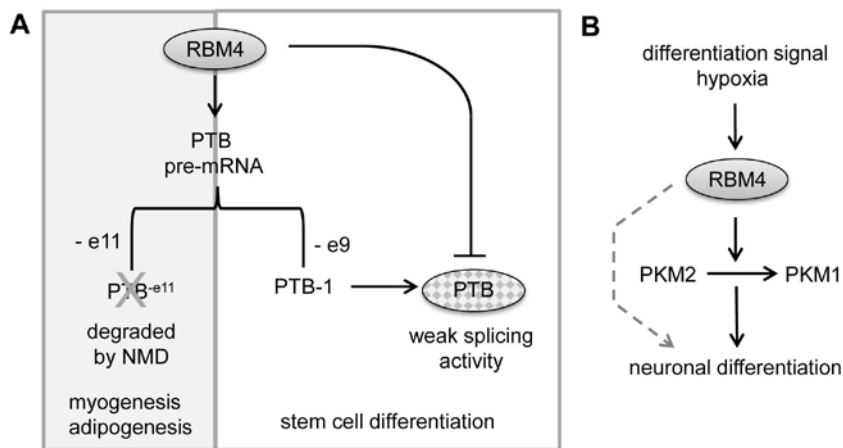


Figure 18. RBM4 modulates neuronal differentiation via alternative splicing regulation. (A) RBM4 modulates alternative splicing of PTB. During myogenesis and adipogenesis, RBM4 promotes the expression of the exon 11-skipped PTB transcript, which is subsequently degraded by NMD. In stem cells, RBM4 induces the skipping of exon 9, resulting in a transcript coding for a functional PTB protein isoform; this isoform exhibits weaker splicing activity as compared to the full-length PTB. Moreover, RBM4 suppresses the activity of PTB in splicing regulation. (B) Cell differentiation signals or hypoxic treatment can induce RBM4 expression. RBM4 promotes the PKM isoform switch towards PKM1, which increases the mitochondrial respiratory capacity and facilitates neuronal differentiation. The possibility remains that RBM4 promotes neuronal differentiation of MSCs via other pathways (dashed line).



Table 1. Primer sequences

Name	Forward (5' to 3')	Reverse (5' to 3')	Species
mRNA expression			
GAPDH	GTCGTGGAGTCTACTGGTGT	TACTTGGCAGGTTTCTCCAG	Mouse
PKM1	CTGGCTCAGAAGATGATGATCG	CATGAGGTCTGTGGAGTGACTGG	
PKM2	CTGGCTCAGAAGATGATGATCG	CTTGGTGAGCACGATAATGG	
RBM4A	CTGCTGCTGCTGCAGCTCCTGAAGG	ATGGTGAAGCTGTTCATTGG	
RBM4B	ATGGTGAAGCTGTTCATTGG	CGGGAAGCACAGCCGCATTC	
β-actin	GCACTCTTGCAGCCTTCCTTCC	TGTCACCTTCACCGTTCCAG	Human
BMP2	ACCCGCTGTCTTCTAGCG	TTTCAGGCCGAACATGCTGAG	
BMP8B	AGGTGGCTTCCTTATCTGCG	ATGTGCCAACTCTGCTTCGT	
HES1	TGAAGAAAGATAGCTCGCGG	CATTGATCTGGGTCATGCAG	
Id1	GGTGCGCTGTCTGTCTGAG	CTGATCTCGCCGTTGAGG	
Id3	CTGGACGACATGAACCACTG	GTAGTCGATGACGCGCTGTA	
MAP2	CTTCAGCTTGTCTCTAACCGAG	CCTTTGCTTCATCTTTCCGTTT	
NURR1	CAATGCGTTCGTGGCTTTGG	GGTACGAAGTTCTGGGAGC	
OCT4	AGCGAACCAGTATCGAGAAC	TTACAGAACCACACTCGGAC	
PKM1	CCTTGCTCAGAAGATGATGATTGG	CATGAGGTCTGTGGAGTGACTTG	

(Continued in next page)

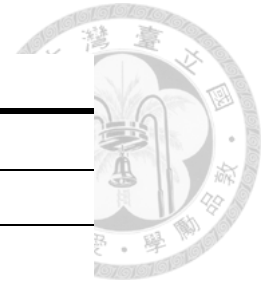


Table 1. Primer sequences (Continued)

Name	Forward (5' to 3')	Reverse (5' to 3')	Species
mRNA expression			
PKM2	CCTTGCTCAGAAGATGATGATTGG	CTTGGTGAGGACGATTATGG	Human
PTB	AAGAGCCGTGACTACACACGC	TTGCCGTCCGCCATCTGCACTA	
RBM4A	GGAATTCTCTGTACGACATGG	GTACCACGAAGGGTGTATTCTC	
RBM4B	GGAATTCTCTGTATGACATGG	CGCGGAGCAAGTTCT	
SNCA	AGGACTTTCAAAGGCCAAGG	TCCTCCAACATTTGTCACTTG	
SOX2	AGCTACAGCATGATGCAGGA	GGTCATGGAGTTGTACTGCA	
TUJ1	GGCCAAGGGTCACTACACG	GCAGTCGCAGTTTTTCACACTC	
Minigene assay (SV40 as forward primer)			
PKM1	CCAAAAAGAAGAGAAAGGTG	CATGAGGTCTGTGGAGTGACTGG	Mouse
PKM2	CCAAAAAGAAGAGAAAGGTG	CTTGGTGAGCACGATAATGG	Mouse
PTB	CCAAAAAGAAGAGAAAGGTG	TGCTGACCAGCAATACAG	Human
Expression vector construct			
FLAG-PKM	GAATTCATGTCGAAGCCCCATAGTGA	CTCGAGTCACGGCACAGGAACAACAC	Human
FLAG-PTB	ACGGAATTCATGGACGGCATTGTCC	ACGGCGGCCCGCCTAGATGGTGGACTTGG	

(Continued in next page)



Table 1. Primer sequences (Continued)

Name	Forward (5' to 3')	Reverse (5' to 3')	Species
EMSA probe construct			
CU rich	CATGTGTTGTCTCTCTTGTTTTTG	GGTTTAGGGTAGGAGGGATAAGG	Mouse
CU poor	GGAGGCTGAGGCAAAGAAAATAGTG	CCTATCAGCCTTGA ACTTGCCAC	
Immunoprecipitation			
PKM	CCTTGCTCAGAAGATGATGATTGG	GATAGTCCCCTTTGACTGTTTCTC	Human
PTB	CAGGAAATTCTGTATTGCT	TTGCCGTCCGCCATCTGCACTA	
U6	CTCGCTTCGGCAGCACA	AACGCTTCACGAATTTGCGT	